Advances in Materials Research, *Vol. 6, No. 2 (2017) 93-128*
DOI: https://doi.org/10.12989/amr.2017.6.2.093

Thermal-induced nonlocal vibration characteristics of heterogeneous beams

Farzad Ebrahimi* and Mohammad Reza Barati

Department of Mechanical Engineering, Faculty of Engineering, Imam Khomeini International University, Qazvin, P.O.B. 16818-34149, Iran

(Received April 18, 2017, Revised May 25, 2017, Accepted May 29, 2017)

Abstract. In this paper, thermal vibration behavior of nanoscale beams made of functionally graded (FG) materials subjected to various types of thermal loading are investigated. A Reddy shear deformation beam theory which captures both the microstructural and shear deformation effects without the need for any shear correction factors is employed. Material properties of FG nanobeam are assumed to be temperature-dependent and vary gradually along the thickness according to the power-law form. The influence of small scale is captured based on nonlocal elasticity theory of Eringen. The nonlocal equations of motion are derived through Hamilton's principle and they are solved applying analytical solution. The comparison of the obtained results is conducted with those of nonlocal Euler-Bernoulli beam theory and it is demonstrated that the proposed modeling predict correctly the vibration responses of FG nanobeams. The effects of nonlocal parameter, material graduation, mode number, slenderness ratio and thermal loading on vibration behavior of the nanobeams are studied in detail.

Keywords: third-order shear deformation beam theory; thermo-mechanical vibration; functionally graded nanobeam; Eringen elasticity theory

1. Introduction

Functionally graded materials (FGMs) are known as modern inhomogeneous composite materials which have gained wide potential applications for various machineries and in various systems and devices under thermo-mechanical loadings, such as heat engine components, spacecraft heat shields, jet fighter structures, and plasma coatings for fusion reactors. In these novel materials, the volume fractions of two or more material constituents such as a pair of ceramic and metal are supposed to change continuously throughout the desired directions. The FGM materials constituents provide several beneficial features, for instance, the ceramic constituents are capable to endure vigorous temperature environments due to their better thermal resistance characteristics, while the metal constituents possess stronger mechanical performance and diminishes the possibility of disastrous fracture. Hence, presenting novel mechanical properties, FGMs have gained its applicability in several engineering fields, such as biomedical

*Corresponding author, Professor, E-mail: febrahimy@gmail.com

 ISSN: 2234-0912 (Print), 2234-179X (Online)

engineering, nuclear engineering and mechanical engineering. Based on these advantages, a number of researches, dealing with static, buckling, dynamic characteristics of FG structures, had been published in the scientific literature (Ebrahimi and Rastgoo 2008a, b, c, Ebrahimi 2013, Ebrahimi *et al.* 2008, 2009a, b, 2016a, Ebrahimi and Zia 2015, Ebrahimi and Mokhtari 2015).

Due to the awesome mechanical, chemical, and electronic properties of structural elements such as nanoscale beams and plates in micro/nano electro-mechanical systems (MEMS/NEMS), a motivation occurred in analysis of micro/nano structures where the size effects are prominent. In these applications, size effects become prominent. Since the invention of carbon nanotubes (CNTs) by Iijima (1999), nanoscale engineering materials have exposed to considerable attention in modern science and technology. These structures possess extraordinary mechanical, thermal, electrical and chemical performances that are superior to the conventional structural materials. Therefore nanostructures attract great interest by researchers based on molecular dynamics and continuum mechanics. The problem in using the classical theory is that the classical continuum mechanics theory does not take into account the size effects in micro/nano scale structures. The classical continuum mechanics over predicts the responses of micro/nano structures. An alternative approach to capture the size effects is using molecular dynamic simulations (MD) which is an accurate implement for analyzing of nano-structural components. But even the molecular dynamic simulation at nano scale is computationally exorbitant for modeling the nanostructures with large numbers of atoms. So a conventional form of continuum mechanics that can capture the small scale effect is required. Eringen's nonlocal elasticity theory (Eringen 1983) is the most commonly used continuum mechanics theory that includes small scale effects with good accuracy to model micro/nano scale devices and systems. The nonlocal elasticity theory assumes that the stress state at a reference point is a function of the strain at all neighbor points of the body. Hence, this theory could take into consideration the effects of small scales. Lots of studies have been performed to investigate the size-dependent response of structural systems based on Eringen's nonlocal elasticity theory (Ebrahimi and Salari 2015a, b, 2016, Ebrahimi *et al.* 2015a, 2016c, Ebrahimi and Nasirzadeh 2015, Ebrahimi and Barati 2016a, b, c, d, e, f, Ebrahimi and Hosseini 2016a, b, c).

In order to investigate as well as design the FG micro and nanoscale structures several studies is conducted in recent years. Concerning taking into account the size-effect for FG beam structures based on the nonlocal constitutive relation of Eringen, a large number of studies have been conducted attempting to develop nonlocal beam models for predicting the mechanical responses of nanobeams. Peddieson *et al.* (2003) proposed the nonlocal Euler-Bernoulli beam theory to be applied to materials in micro and nano scale. Various available beam theories are formulated by Reddy (2007), through nonlocal differential relations of Eringen. A general nonlocal beam model for analysis bending, buckling, and vibration of nanobeams using different beam theories are presented by Aydogdu (2009). The flapwise bending-vibration of rotating nanocantilevers are investigated by Pradhan and Murmu (2010) using differential quadrature method. They noticed that size effects have a main role in the vibration behavior of rotating nanostructures. Thai (2012) suggested a nonlocal higher order beam theory to study mechanical responses of nanobeams. Civalek *et al.* (2010) proposed formulation of the governing equations of nonlocal Euler-Bernoulli beams to investigate bending of cantilever microtubules via the differential quadrature method. In other scientific work, Wang and Liew (2007) carried out the static analysis of micro and nano scale structures based on nonlocal continuum mechanics using Euler-Bernoulli and Timoshenko beam theory. Simsek (2014) proposed a non-classical beam model based on the Eringen's nonlocal elasticity theory for nonlinear vibration of nanobeams with various boundary conditions. The nonlocal beam model based on Eringen's theory for the vibration of FG and composite nanobeams are presented by Zenkour *et al.* (2014). Ansari *et al.* (2015) investigate a size-dependent nonlinear forced vibration of magneto-electro-thermo-elastic Timoshenko nanobeams based on the nonlocal elasticity theory.

To properly apply the FG micro/nano materials in micro/nano electromechanical systems (MEMS/NEMS), their mechanical behavior needs to be investigated. Recently, Eltaher *et al.* (2012) presented a finite element analysis for free vibration of FG nanobeams using nonlocal EBT. Rahmani and Pedram (2014) analyzed the size effects on vibration of FG nanobeams based on nonlocal TBT. Also, recently Hosseini-Hashemi *et al.* (2014) investigated free vibration of FG nanobeams with consideration surface effects and piezoelectric field using nonlocal elasticity theory. Ebrahimi *et al.* (2015) and Ebrahimi and Salari (2015a) examined the applicability of differential transformation method in investigations on vibrational characteristics of FG size-dependent nanobeams. Most recently Ebrahimi and Barati (2016g, h, I, j, k, l, m, n, o, p, q, r, s, t, u, v, 2017a, b) and Ebrahimi *et al.* (2017) explored thermal and hygro-thermal effects on nonlocal behavior of FG nanobeams and nanoplates. Li and Hu (2017) examined torsional vibration of bi-directional functionally graded nanotubes based on nonlocal elasticity theory. Also, they (2017) performed post-buckling analysis of functionally graded nanobeams incorporating nonlocal stress and microstructure-dependent strain gradient effects. Li *et al.* (2016) carried out free vibration analysis of nonlocal strain gradient beams made of functionally graded material.

Although the size-dependent FG beam models have been developed in the aforementioned studies, most of them ignore the effects of thermal environment. Also, the common use of FGMs in high temperature environment leads to considerable changes in material properties. For example, Young's modulus usually reduces when temperature increases in FGMs. To predict the behavior of FGMs subjected to extreme temperatures more accurately, it is necessary to consider the temperature dependency on material constituent's properties. Furthermore, due to the expansion of new industries and technologies, many systems and structures experience severe thermal environments, resulting in various types of thermal loads. This situation has created a need for a text that is focused on the analysis of thermal vibration. Thermal vibration is a phenomenon in many structures that should be checked to ensure the safety of structures. Consequently, thermal vibration analysis of beam structures is common in structural mechanics. Hence, presenting an accurate model of FG nanobeams is very important for successful NEMS design. Considering great application of beams in different engineering fields such as aerospace and mechanical engineering, and due to the fact that making temperatures and working temperature of structures are not equal, for more accurate design, it is useful to study their thermos-mechanical behavior. Several studies have been performed to investigate the thermal effect on mechanical responses of FGM beams. Wattanasakulpong *et al.* (2011) investigated thermal buckling and elastic vibration of third-order shear deformable FG beams. Thermo-mechanical buckling and nonlinear free vibration analysis of FG beams on nonlinear elastic foundation is investigated by Fallah and Aghdam (2012). Small amplitude vibrations of a FG material beam under in-plane thermal loading in the prebuckling and postbuckling regimes is studied by Esfahani *et al.* (2014). It should be cited that, in these work the beams are in macro scale and small scale effect is not taken into consideration. For the FG nanobeam problems, Ebrahimi and Salari (2015c) investigated the thermal effects on buckling and free vibration characteristics of FG size-dependent Timoshenko nanobeams subjected to an in-plane thermal loading. In another study, Thermo-mechanical vibration analysis of nonlocal temperature-dependent FG nanobeams with various boundary conditions is investigated by Ebrahimi and Salari (2015d). An exact solution for the nonlinear forced vibration of FG nanobeams in thermal environment based on surface elasticity theory is presented by Ansari *et al.*

(2015). It is noticed that most of the previous studies on mechanical analysis of FG nanobeams have been carried out based on Euler-Bernoulli and Timoshenko beam theories. It should be noted that the EBT fails to consider the influences of shear deformations. This theory is only applicable for slender beams and should not be applied for thick beams, and also it suppose that the transverse perpendicular to the neutral surface stays normal during and after bending, which indicates that the transversal shear strain is equal to zero Hence, the buckling loads and natural frequencies of thick beams are overestimated in which shear deformation effects are prominent. Timoshenko Beam Theory can enumerate the influences of shear deformations for thick beams with presumption of a constant shear strain state in the direction of beam thickness. So, as a disadvantage of this theory, a shear correction factor is required to properly demonstration of the deformation strain energy. To prevent using the shear correction factors, many higher-order shear deformation theories have been developed such as the third-order shear deformation theory proposed by Reddy (2007), the generalized beam theory proposed by Aydogdu (2009) and sinusoidal shear deformation theory of Touratier (1991). Reddy's third order beam theory (RBT) can be used with supposing the higher order longitudinal displacement variations of beam along the thickness. By verifying zero transverse shear stresses at the upper and lower surfaces of the beam, this theory captures both the microstructural and shear deformation effects. Therefore, The Reddy beam theory is more exact and provides better representation of the physics of the problem, which does not need any shear correction factors. This theory relaxes the limitation on the warping of the cross sections and allows cubic variations in the longitudinal direction of the beam, so it can produce adequate accuracy when applying for beam analysis. Therefore, a few numbers of studies have been conducted to investigate the mechanical responses of FG micro/nano beams by using higher shear deformation beam theories. Sahmani *et al.* (2015) investigated the free vibration response of third-order shear deformable nanobeams made of FGMs around the postbuckling domain incorporating the effects of surface free energy. Zhang *et al.* (2005) developed a size-dependent FG beam model resting on Winkler-Pasternak elastic foundation based on an improved third-order shear deformation theory and provided the analytical solutions for the bending, buckling and free vibration problems. By searching the literature, it is found that a work analyzing the thermal vibration of FG nanobeams using the third-order shear deformation beam theory hasn't been yet published.

In the present work, thermo-mechanical vibrational behavior of the higher-order FG nanobeams in thermal environment are investigated applying Navier analytical method. The FG nanobeam is supposed to be exposed under three types of thermal loads including uniform, linear and nonlinear temperature changes. Thermo-mechanical properties of the FG nanobeams are both temperature-dependent and position-dependent. The nonlocal governing differential equations in thermal environment are derived by implementing Hamilton's principle and using nonlocal constitutive equations of Eringen. Accuracy of the results is examined using available date in the literature. The effects of small scale parameter, material graduation, thermal loading and slenderness ratio on thermal vibration of FG nanobeams are investigated.

2. Governing equations

2.1 Power-law functionally graded material (P-FGM) beam

One of the most favorable models for FGMs is the power-law model, in which material

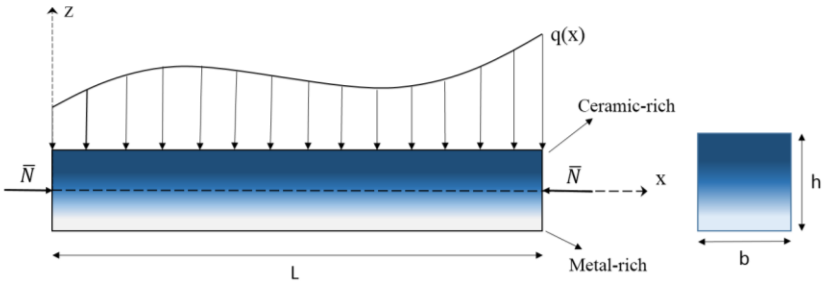

Fig. 1 Geometry and coordinates of FG nanobeam

properties of FGMs are supposed to change according to a power law about spatial coordinates. The coordinate system for FG nano beam is shown in Fig. 1.

The FG nanobeam is assumed to be combination of ceramic and metal and effective material properties (P_f) of the FG beam such as Young's modulus E_f and mass density ρ are supposed to change continuously in the direction of z-axis (thickness direction) according to an power function of the volume fractions of the material constituents. So, the effective material properties, P_f can be stated as

$$P_f = P_c V_c + P_m V_m, \tag{1}$$

where subscripts m and c denote metal and ceramic, respectively and the volume fraction of the ceramic is associated to that of the metal in the following relation

$$V_c + V_m = 1. \tag{2a}$$

The volume fraction of the ceramic constituent of the beam is assumed to be given by

$$V_c = \left(\frac{z}{h} + \frac{1}{2}\right)^p, \tag{2b}$$

Here p is the power-law exponent which determines the material distribution through the thickness of the beam and z is the distance from the mid-plane of the FG nanobeam. Therefore from Eqs. (1) and (2), the effective material properties of the FG nanobeam such as Young's modulus (E), mass density (ρ), Poisson's ratio (ν), coefficient of thermal expansion (α_t) and thermal conductivity (κ) can be expressed as follows

$$\begin{Bmatrix} E(z) \\ \rho(z) \\ \nu(z) \\ \alpha_t(z) \\ \kappa(z) \end{Bmatrix} = \begin{Bmatrix} E_c - E_m \\ \rho_c - \rho_m \\ \nu_c - \nu_m \\ \alpha_c - \alpha_m \\ \kappa_c - \kappa_m \end{Bmatrix} \left(\frac{z}{h} + \frac{1}{2}\right)^p + \begin{Bmatrix} E_m \\ \rho_m \\ \nu_m \\ \alpha_m \\ \kappa_m \end{Bmatrix}. \tag{3}$$

The material composition of FG nanobeam at the upper surface ($z = +h/2$) is supposed to be the pure ceramic and it changes continuously to the opposite side surface ($z = -h/2$) which is pure metal. To more accurate prediction of FGMs behavior under high temperature, it is necessary to consider the temperature dependency on material properties. The nonlinear equation of thermo-elastic material properties in function of temperature T(K) can be expressed as Ebrahimi and Salari (2015c)

Table 1 Temperature dependent coefficients for Si_3N_4 and SUS304

Material	Properties	P_0	P_{-1}	P_1	P_2	P_3
Si_3N_4	E(Pa)	348.43e+9	0	-3.070e-4	2.160e-7	-8.946e-11
	α(K^{-1})	5.8723e-6	0	9.095e-4	0	0
	ρ(Kg/m^3)	2370	0	0	0	0
	κ(W/mK)	13.723	0	-1.032e-3	5.466e-7	-7.876e-11
	ν	0.24	0	0	0	0
SUS304	E(Pa)	201.04e+9	0	3.079e-4	-6.534e-7	0
	α(K^{-1})	12.330e-6	0	8.086e-4	0	0
	ρ(Kg/m^3)	8166	0	0	0	0
	κ(W/mK)	15.379	0	-1.264e-3	2.092e-6	-7.223e-10
	ν	0.3262	0	-2.002e-4	3.797e-7	0

$$P = P_0(P_{-1}T^{-1} + 1 + P_1T + P_2T^2 + P_3T^3), \tag{4}$$

where P_0, P_{-1}, P_1, P_2 and P_3 are the temperature dependent coefficients of temperature, T(K) which can be seen in the Table 1 that contains material properties of Si_3N_4 and SUB304.

2.2 Kinematic relations

Based on the third order shear deformation (Reddy) beam theory, the displacement field at any point of the beam can be written as

$$\begin{gathered} u_x(x,z) = u(x) + z\varphi(x) - \alpha z^3\left(\varphi + \frac{\partial w}{\partial x}\right), \\ u_z(x,z) = w(x), \end{gathered} \tag{5}$$

where $\alpha = \frac{4}{3h^2}$ and u and w are the longitudinal and the transverse displacements, φ is the rotation of the cross section at each point of the neutral axis. Nonzero strains of the Reddy beam model are expressed as follows

$$\varepsilon_{xx} = \varepsilon_{xx}^{(0)} + z\varepsilon_{xx}^{(1)} + z^3\varepsilon_{xx}^{(3)}, \quad \gamma_{xz} = \gamma_{xz}^{(0)} + z^2\gamma_{xz}^{(2)}. \tag{6}$$

where

$$\begin{gathered} \varepsilon_{xx}^{(0)} = \frac{\partial u}{\partial x}, \quad \varepsilon_{xx}^{(1)} = \frac{\partial \varphi}{\partial x}, \quad \varepsilon_{xx}^{(3)} = -\alpha\left(\frac{\partial \varphi}{\partial x} + \frac{\partial^2 w}{\partial x^2}\right), \\ \gamma_{xz}^{(0)} = \varphi + \frac{\partial w}{\partial x}, \quad \gamma_{xz}^{(2)} = -\beta\left(\varphi + \frac{\partial w}{\partial x}\right), \end{gathered} \tag{7}$$

and $\beta = \frac{4}{h^2}$. By using the Hamilton's principle, in which the motion of an elastic structure in the time interval $t_1 < t < t_2$ is so that the integral with respect to time of the total potential energy is extremum

$$\int_0^t \delta(K-U-V)\mathrm{d}t = 0, \tag{8}$$

where K is the kinetic energy, U is the total strain energy and V is the work done by external forces. The virtual strain energy can be calculated as

$$\delta U = \iiint_{\mathrm{v}} \sigma_{ij}\delta\varepsilon_{ij}\mathrm{dv} = \iiint_{\mathrm{v}} (\sigma_{xx}\delta\varepsilon_{xx} + \sigma_{xz}\delta\gamma_{xz})\mathrm{dv}. \tag{9}$$

Substituting Eq. (6) into Eq. (9) yields

$$\delta U = \int_0^L \left(N\delta\varepsilon_{xx}^{(0)} + M\delta\varepsilon_{xx}^{(1)} + P\delta\varepsilon_{xx}^{(3)} + Q\delta\gamma_{xz}^{(0)} + R\delta\gamma_{xz}^{(2)}\right)\mathrm{d}x. \tag{10}$$

in which the variables introduced in arriving at the last expression are defined as follows

$$\begin{gathered} \{N, M, P\} = \iint_A \sigma_{xx}\{1, z, z^3\}\mathrm{d}A\,, \\ \{Q, R\} = \iint_A \sigma_{xz}\{1, z^2\}\mathrm{d}A\,, \end{gathered} \tag{11}$$

The first variation of the work done by applied forces can be written in the form

$$\delta V = \int_0^L \left[\left(N^T\frac{\partial w}{\partial x}\frac{\partial}{\partial x} + q + \alpha P\frac{\partial^2}{\partial x^2}\right)\delta w + f\delta u - N\delta\varepsilon_{xx}^{(0)} - \bar{M}\frac{\partial\delta\varphi}{\partial x} - \bar{Q}\delta\gamma_{xz}^{(0)}\right]\mathrm{d}x, \tag{12}$$

where N^T is thermal resultant, $\bar{M} = M - \alpha P$, $\bar{Q} = Q - \beta R$ and $\mathcal{N}$ is the applied axial compressive load and $q(x)$ and $f(x)$ are the transverse and axial distributed loads and k_W and k_P are linear and shear coefficient of elastic foundation. The thermal resultant can be expressed as

$$N^T = \int_{-h/2}^{h/2} E(z,T)\alpha_t(z,T)(T-T_0)\mathrm{d}z. \tag{13}$$

The first variation of the virtual kinetic energy can be written in the form

$$\begin{gathered} \delta K = \int_0^L \Big\{I_0\left(\frac{\partial u}{\partial t}\frac{\partial\delta u}{\partial t} + \frac{\partial w}{\partial t}\frac{\partial\delta w}{\partial t}\right) + I_1\left(\frac{\partial u}{\partial t}\frac{\partial\delta\varphi}{\partial t} + \frac{\partial\varphi}{\partial t}\frac{\partial\delta u}{\partial t}\right) + I_2\frac{\partial\varphi}{\partial t}\frac{\partial\delta\varphi}{\partial t} - \alpha\Big[I_3\frac{\partial u}{\partial t}\Big(\frac{\partial^2\delta w}{\partial x\partial t} + \\ \frac{\partial\delta\varphi}{\partial t}\Big) + I_3\frac{\partial\delta u}{\partial t}\Big(\frac{\partial^2 w}{\partial x\partial t} + \frac{\partial\varphi}{\partial t}\Big) + I_4\frac{\partial\varphi}{\partial t}\left(\frac{\partial^2\delta w}{\partial x\partial t} + \frac{\partial\delta\varphi}{\partial t}\right) + I_4\frac{\partial\delta\varphi}{\partial t}\left(\frac{\partial^2 w}{\partial x\partial t} + \frac{\partial\varphi}{\partial t}\right) - \alpha I_6\Big(\frac{\partial^2 w}{\partial x\partial t} + \\ \frac{\partial\varphi}{\partial t}\Big)\left(\frac{\partial^2\delta w}{\partial x\partial t} + \frac{\partial\delta\varphi}{\partial t}\right)\Big\}\mathrm{d}x, \end{gathered} \tag{14}$$

where I_j represent the mass inertia

$$I_j = \iint_A \rho z^j\mathrm{d}A. \tag{15}$$

It is to be noted that for homogeneous nanobeams we have $I_1 = I_3 = 0$.

By substituting Eqs. (10), (12) and (14) into Eq. (8) and setting the coefficients of δu, δw and $\delta\varphi$ to zero, the following Euler-Lagrange equation can be obtained

$$\begin{gathered} \frac{\partial N}{\partial x} + f = I_0\frac{\partial^2 u}{\partial t^2} + \hat{I}_1\frac{\partial^2\varphi}{\partial t^2} - \alpha I_3\frac{\partial^3 w}{\partial x\partial t^2}, \\ \frac{\partial\bar{M}}{\partial x} - \bar{Q} = \hat{I}_1\frac{\partial^2 u}{\partial t^2} + \hat{I}_2\frac{\partial^2\varphi}{\partial t^2} - \alpha\hat{I}_4\left(\frac{\partial^3 w}{\partial x\partial t^2} + \frac{\partial^2\varphi}{\partial t^2}\right), \\ \frac{\partial\bar{Q}}{\partial x} - \frac{\partial}{\partial x}\left(N^T\frac{\partial w}{\partial x}\right) + \alpha\frac{\partial^2 P}{\partial x^2} + q = I_0\frac{\partial^2 w}{\partial t^2} + \alpha I_3\frac{\partial^3 u}{\partial x\partial t^2} + \alpha I_4\frac{\partial^3\varphi}{\partial x\partial t^2} - \alpha^2 I_6\left(\frac{\partial^4 w}{\partial x^2\partial t^2} + \frac{\partial^3\varphi}{\partial x\partial t^2}\right) \end{gathered} \tag{16}$$

where $\hat{I}_j = I_j - \alpha I_{j+2}$.

2.3 The nonlocal elasticity model for FG nanobeam

According to Eringen nonlocal elasticity model, the stress state at a point inside a body is regarded to be function of strains of all points in the neighbor regions. For homogeneous elastic solids the nonlocal stress-tensor components σ_{ij} at each point x in the solid can be defined as

$$\sigma_{ij}(x) = \iiint_{\mathrm{V}} \psi(|x - x'|, \tau) t_{ij}(x') \mathrm{dv}(x'), \tag{17}$$

where $t_{ij}(x')$ are the components available in local stress tensor at point x which are associated to the strain tensor components ε_{kl} as

$$t_{ij} = C_{ijkl}\varepsilon_{kl}. \tag{18}$$

The concept of Eq. (17) is that the nonlocal stress at any point is weighting average of local stress of all points in the near region that point, the size that is related to the nonlocal kernel $\psi(|x - x'|, \tau)$. Also $|x - x'|$ is Euclidean distance and τ is a constant given by

$$\tau = \frac{e_0 a}{l}. \tag{19}$$

which indicates the relation of a characteristic internal length, (for instance lattice parameter, C-C bond length and granular distance) and a characteristic external length, l (for instance crack length and wavelength) using a constant, e_0, dependent on each material. The value of e_0 is experimentally estimated by comparing the scattering curves of plane waves and atomistic dynamics. According to (Eringen 1983) for a class of physically admissible kernel $\psi(|x - x'|, \tau)$. It is possible to represent the integral constitutive relations given by Eq. (17) in an equivalent differential form as

$$[1 - (e_0 a)^2 \nabla^2]\sigma_{kl} = t_{kl}, \tag{20}$$

where ∇^2 is the Laplacian operator. Thus, the scale length $e_0 a$ consider the influences of small scales on the response of nano-structures. The magnitude of the small scale parameter relies on several parameters including mode shapes, boundary conditions, chirality and the essence of motion. The parameter $e_0 = (\pi^2 - 4)^{1/2}/2\pi \cong 0.39$ was given by Eringen (1983). Also, Zhang *et al.* (2005) found the value of 0.82 nm for nonlocal parameter when they compared the vibrational results of simply supported single-walled carbon nanotubes with molecular dynamics simulations. The nonlocal parameter, μ, is experimentally obtained for various materials; for instance, a conservative estimate of $\mu < 4$ (nm)^2 for a single-walled carbon nanotube is proposed (Wang and Hu 2005). It is worth mentioning that this magnitude is dependent of size and chirality, because the properties of carbon nanotubes are extensively confirmed to be dependent of chirality. There is no serious study conducted to determining the value of small scale to simulate mechanical behavior of FG micro/nanobeams. Hence all researchers who worked on size-dependent mechanical behavior of FG nanobeams on the basis the nonlocal elasticity method investigated the influence of small scale parameter on mechanical behavior of FG nanobeams by changing the value of the small scale parameter. In the present work, the nonlocal parameter is assumed to be in the range of 0-5 (nm)^2 (Eltaher *et al.* 2012). So, for a material in the one-dimension case, the constitutive relations of nonlocal theory can be expressed as

$$\begin{aligned} \sigma_{xx} - (e_0 a)^2 \frac{\partial^2 \sigma_{xx}}{\partial x^2} &= E\varepsilon_{xx}, \\ \sigma_{xz} - (e_0 a)^2 \frac{\partial^2 \sigma_{xz}}{\partial x^2} &= G\gamma_{xz}, \end{aligned} \tag{21}$$

where σ and ε are the nonlocal stress and strain, respectively. E is the Young's modulus, $G(z) = \frac{E(z)}{2[1+\nu(z)]}$ is the shear modulus (where ν is the Poisson's ratio). For a nonlocal FG beam, Eq. (21) can be written as

$$\begin{aligned} \sigma_{xx} - \mu \frac{\partial^2 \sigma_{xx}}{\partial x^2} &= E(z)\varepsilon_{xx}, \\ \sigma_{xz} - \mu \frac{\partial^2 \sigma_{xz}}{\partial x^2} &= G(z)\gamma_{xz}, \end{aligned} \tag{22}$$

where ($\mu = (e_0 a)^2$). Integrating Eq. (22) over the beam's cross-section area, we obtain the force-strain and the moment-strain of the nonlocal Reddy FG beam theory can be obtained as follows

$$N - \mu \frac{\partial^2 N}{\partial x^2} = A_{xx} \frac{\partial u}{\partial x} + (B_{xx} - \alpha E_{xx}) \frac{\partial \varphi}{\partial x} - \alpha E_{xx} \frac{\partial^2 w}{\partial x^2}, \tag{23}$$

$$M - \mu \frac{\partial^2 M}{\partial x^2} = B_{xx} \frac{\partial u}{\partial x} + (D_{xx} - \alpha F_{xx}) \frac{\partial \varphi}{\partial x} - \alpha F_{xx} \frac{\partial^2 w}{\partial x^2}, \tag{24}$$

$$P - \mu \frac{\partial^2 P}{\partial x^2} = E_{xx} \frac{\partial u}{\partial x} + (F_{xx} - \alpha H_{xx}) \frac{\partial \varphi}{\partial x} - \alpha H_{xx} \frac{\partial^2 w}{\partial x^2}, \tag{25}$$

$$Q - \mu \frac{\partial^2 Q}{\partial x^2} = (A_{xz} - \beta D_{xz}) \left(\frac{\partial w}{\partial x} + \varphi \right), \tag{26}$$

$$R - \mu \frac{\partial^2 R}{\partial x^2} = (D_{xz} - \beta F_{xz}) \left(\frac{\partial w}{\partial x} + \varphi \right), \tag{27}$$

in which the cross-sectional rigidities are defined as follows

$$\{A_{xx}, B_{xx}, D_{xx}, E_{xx}, F_{xx}, H_{xx}\} = \int_{-h/2}^{h/2} E(z)\{1, z, z^2, z^3, z^4, z^6\} \mathrm{d}z, \tag{28}$$

$$\{A_{xz}, D_{xz}, F_{xz}\} = \int_{-h/2}^{h/2} G(z)\{1, z^2, z^4\} \mathrm{d}z. \tag{29}$$

The explicit relation of the nonlocal normal force can be derived by substituting for the second derivative of N from Eq. $(16)_1$ into Eq. (23) as follows

$$N = A_{xx} \frac{\partial u}{\partial x} + K_{xx} \frac{\partial \varphi}{\partial x} - \alpha E_{xx} \frac{\partial^2 w}{\partial x^2} + \mu \left(I_0 \frac{\partial^3 u}{\partial x \partial t^2} + \hat{I}_1 \frac{\partial^3 \varphi}{\partial x \partial t^2} - \alpha I_3 \frac{\partial^4 w}{\partial t^2 \partial t^2} - \frac{\partial f}{\partial x} \right). \tag{30}$$

Eliminating $\bar{Q}$ from Eqs. $(16)_2$ and $(16)_3$, we obtain the following equation

$$\frac{\partial^2 \bar{M}}{\partial x^2} = \frac{\partial}{\partial x}\left(N^T \frac{\partial w}{\partial x}\right) - \alpha \frac{\partial^2 P}{\partial x^2} - q + I_0 \frac{\partial^2 w}{\partial t^2} + I_1 \frac{\partial^3 u}{\partial x \partial t^2} + I_2 \frac{\partial^3 \varphi}{\partial x \partial t^2} - \alpha I_4 \left(\frac{\partial^4 w}{\partial x^2 \partial t^2} + \frac{\partial^3 \varphi}{\partial x \partial t^2}\right). \tag{1}$$

Also the explicit relation of the nonlocal bending moment can be derived by substituting the above equations into Eqs. (24) and (25) as follows

$$\bar{M} = K_{xx} \frac{\partial u}{\partial x} + \bar{I}_{xx} \frac{\partial \varphi}{\partial x} - \alpha J_{xx} \frac{\partial^2 w}{\partial x^2} + \mu \left[\frac{\partial}{\partial x}\left(N^T \frac{\partial w}{\partial x}\right) - \alpha \frac{\partial^2 P}{\partial x^2} - q + I_0 \frac{\partial^2 w}{\partial t^2} + I_1 \frac{\partial^3 u}{\partial x \partial t^2} + I_2 \frac{\partial^3 \varphi}{\partial x \partial t^2} - \alpha I_4 \left(\frac{\partial^4 w}{\partial x^2 \partial t^2} + \frac{\partial^3 \varphi}{\partial x \partial t^2}\right)\right], \tag{32}$$

where

$$K_{xx} = B_{xx} - \alpha E_{xx}, \quad I_{xx} = D_{xx} - \alpha F_{xx}, \quad J_{xx} = F_{xx} - \alpha H_{xx}, \quad \bar{I}_{xx} = I_{xx} - \alpha J_{xx}. \tag{33}$$

By substituting for the second derivative of $\bar{Q}$ from Eq. $(16)_3$ into Eq. (26) with the aid of Eq. (27) the following expression for the nonlocal shear force will be derived

$$\bar{Q} = A_{xz}^* \left(\frac{\partial w}{\partial x} + \varphi\right) + \mu \left[\frac{\partial^2}{\partial x^2}\left(N^T \frac{\partial w}{\partial x}\right) - \alpha \frac{\partial^3 P}{\partial x^3} - \frac{\partial q}{\partial x} + I_0 \frac{\partial^3 w}{\partial x \partial t^2} + \alpha I_3 \frac{\partial^4 u}{\partial x^2 \partial t^2} + \alpha I_4 \frac{\partial^4 \varphi}{\partial x^2 \partial t^2} - \alpha^2 I_6 \left(\frac{\partial^5 w}{\partial x^3 \partial t^2} + \frac{\partial^4 \varphi}{\partial x^2 \partial t^2}\right)\right], \tag{34}$$

where

$$A_{xz}^* = \bar{A}_{xz} - \beta \bar{D}_{xz}, \quad \bar{A}_{xz} = A_{xz} - \beta D_{xz}, \quad \bar{D}_{xz} = D_{xz} - \beta F_{xz}. \tag{35}$$

Now we use $\bar{M}$ and $\bar{Q}$ from Eqs. (32) and (34) and the identity that given from Eq. (25) to get

$$\alpha \frac{\partial^2}{\partial x^2}\left(P - \mu \frac{\partial^2 P}{\partial x^2}\right) = \alpha E_{xx} \frac{\partial^3 u}{\partial x^3} + \alpha J_{xx} \frac{\partial^3 \varphi}{\partial x^3} - \alpha^2 H_{xx} \frac{\partial^4 w}{\partial x^4}. \tag{36}$$

The nonlocal governing equations of third-order shear deformation FG nanobeam in terms of the displacement can be derived by substituting for N, $\bar{M}$ and $\bar{Q}$ from Eqs. (30), (32) and (34), respectively, and using Eq. (36) into Eq. (16) as follows

$$A_{xx} \frac{\partial^2 u}{\partial x^2} + K_{xx} \frac{\partial^2 \varphi}{\partial x^2} - \alpha E_{xx} \frac{\partial^3 w}{\partial x^3} + f - I_0 \frac{\partial^2 u}{\partial t^2} - \hat{I}_1 \frac{\partial^2 \varphi}{\partial t^2} + \alpha I_3 \frac{\partial^3 w}{\partial x \partial t^2} - \mu \left(\frac{\partial^2 f}{\partial x^2} - I_0 \frac{\partial^4 u}{\partial x^2 \partial t^2} - \hat{I}_1 \frac{\partial^4 \varphi}{\partial x^2 \partial t^2} + \alpha I_3 \frac{\partial^5 w}{\partial x^3 \partial t^2}\right) = 0, \tag{37}$$

$$K_{xx} \frac{\partial^2 u}{\partial x^2} + \bar{I}_{xx} \frac{\partial^2 \varphi}{\partial x^2} - \alpha J_{xx} \frac{\partial^3 w}{\partial x^3} - A_{xz}^* \left(\frac{\partial w}{\partial x} + \varphi\right) - \hat{I}_1 \frac{\partial^2 u}{\partial t^2} - \hat{I}_2 \frac{\partial^2 \varphi}{\partial t^2} + \alpha \hat{I}_4 \left(\frac{\partial^3 w}{\partial x \partial t^2} + \frac{\partial^2 \varphi}{\partial t^2}\right) + \mu \left[\hat{I}_1 \frac{\partial^4 u}{\partial x^2 \partial t^2} + \hat{I}_2 \frac{\partial^4 \varphi}{\partial x^2 \partial t^2} - \alpha \hat{I}_4 \left(\frac{\partial^5 w}{\partial x^3 \partial t^2} + \frac{\partial^4 \varphi}{\partial x^2 \partial t^2}\right)\right] = 0, \tag{38}$$

$$A_{xz}^{*}\left(\frac{\partial^2 w}{\partial x^2}+\frac{\partial \varphi}{\partial x}\right)+\alpha E_{xx}\frac{\partial^3 u}{\partial x^3}+\alpha J_{xx}\frac{\partial^3 \varphi}{\partial x^3}-\alpha^2 H_{xx}\frac{\partial^4 w}{\partial x^4}-\frac{\partial}{\partial x}\left(N^T\frac{\partial w}{\partial x}\right)+q-I_0\frac{\partial^2 w}{\partial t^2}$$
$$-\alpha I_3\frac{\partial^3 u}{\partial x\partial t^2}-\alpha I_4\frac{\partial^3 \varphi}{\partial x\partial t^2}+\alpha^2 I_6\left(\frac{\partial^4 w}{\partial x^2\partial t^2}+\frac{\partial^3 \varphi}{\partial x\partial t^2}\right)+\mu\left[\frac{\partial^3}{\partial x^3}\left(N^T\frac{\partial w}{\partial x}\right)-\frac{\partial^2 q}{\partial x^2}+I_0\frac{\partial^4 w}{\partial x^2\partial t^2}\right. \tag{39}$$
$$\left.+\alpha I_3\frac{\partial^5 u}{\partial x^3\partial t^2}+\alpha I_4\frac{\partial^5 \varphi}{\partial x^3\partial t^2}-\alpha^2 I_6\left(\frac{\partial^6 w}{\partial x^4\partial t^2}+\frac{\partial^5 \varphi}{\partial x^3\partial t^2}\right)\right]=0.$$

3. Solution procedures

Here, on the basis the Navier method, an analytical solution of the governing equations for free vibration of a simply-supported FG nanobeam is presented. To satisfy governing equations of motion and the simply supported boundary condition, the displacement variables are adopted to be of the form

$$\begin{Bmatrix} u(x,t)\\ w(x,t)\\ \varphi(x,t)\end{Bmatrix}=\sum_{n=1}^{\infty}\begin{Bmatrix} U_n\cos\left(\frac{n\pi}{L}x\right)\\ W_n\sin\left(\frac{n\pi}{L}x\right)\\ \Phi_n\cos\left(\frac{n\pi}{L}x\right)\end{Bmatrix}\mathrm{e}^{\mathrm{i}\omega_n t}, \tag{40}$$

where (U_n, W_n, Φ_n) are the unknown Fourier coefficients to be determined for each n value. The boundary conditions for simply-supported beam are given by

$$u(0,t)=0,\quad \left.\frac{\partial u}{\partial x}\right|_{x=L}=0,\quad w(0,t)=w(L,t)=0,\quad \left.\frac{\partial \varphi}{\partial x}\right|_{x=0}=\left.\frac{\partial \varphi}{\partial x}\right|_{x=L}=0. \tag{41}$$

Substituting Eq. (40) into Eqs. (37)-(39), respectively, leads to

$$\left\{I_0\left[1+\mu\left(\frac{n\pi}{L}\right)^2\right]\omega_n^2-A_{xx}\left(\frac{n\pi}{L}\right)^2\right\}U_n+\left\{\hat{I}_1\left[1+\mu\left(\frac{n\pi}{L}\right)^2\right]\omega_n^2-K_{xx}\left(\frac{n\pi}{L}\right)^2\right\}\Phi_n$$
$$+\frac{n\pi}{L}\alpha\left\{E_{xx}\left(\frac{n\pi}{L}\right)^2-I_3\left[1+\mu\left(\frac{n\pi}{L}\right)^2\right]\omega_n^2\right\}W_n=0, \tag{42}$$

$$\left\{\hat{I}_1\left[1+\mu\left(\frac{n\pi}{L}\right)^2\right]\omega_n^2-K_{xx}\left(\frac{n\pi}{L}\right)^2\right\}U_n-\left\{\bar{I}_{xx}\left(\frac{n\pi}{L}\right)^2+A_{xz}^{*}-\hat{I}_2\left[1+\mu\left(\frac{n\pi}{L}\right)^2\right]\omega_n^2\right\}\Phi_n$$
$$+\frac{n\pi}{L}\left\{\alpha J_{xx}\left(\frac{n\pi}{L}\right)^2-A_{xz}^{*}-\alpha\hat{I}_4\left[1+\mu\left(\frac{n\pi}{L}\right)^2\right]\omega_n^2\right\}W_n=0, \tag{43}$$

$$\frac{n\pi}{L}\alpha\left\{E_{xx}\left(\frac{n\pi}{L}\right)^2-I_3\left[1+\mu\left(\frac{n\pi}{L}\right)^2\right]\omega_n^2\right\}U_n$$
$$+\frac{n\pi}{L}\left\{\alpha J_{xx}\left(\frac{n\pi}{L}\right)^2-A_{xz}^{*}-\alpha\hat{I}_4\left[1+\mu\left(\frac{n\pi}{L}\right)^2\right]\omega_n^2\right\}\Phi_n$$
$$\left\{-\left(\frac{n\pi}{L}\right)^2\left[A_{xz}^{*}+\alpha^2 H_{xx}\left(\frac{n\pi}{L}\right)^2\right]\right. \tag{44}$$
$$\left.+\left[1+\mu\left(\frac{n\pi}{L}\right)^2\right]\left[N^T\left(\frac{n\pi}{L}\right)^2+\left(I_0+\alpha^2 I_6\left(\frac{n\pi}{L}\right)^2\right)\omega_n^2\right]\right\}W_n=0.$$

By setting the determinant of the coefficient matrix of the above equations, the analytical solutions can be obtained from the following equations

$$([K] + N^T[K^T] - \omega_n^2[M])\{\Delta\} = \{0\}, \tag{45}$$

where $\{\Delta\} = \{U_n, W_n, \Phi_n\}^T$, $[K]$ is the stiffness matrix, $[K^T]$ is the coefficient matrix of temperature change, and $[M]$ is the mass matrix. By setting this polynomial to zero, we can find natural frequencies ω_n.

4. Types of thermal loading

4.1 Uniform temperature rise (UTR)

For a FG nanobeam at reference temperature T_0 the temperature is uniformly raised to a final value T which the temperature change is $\Delta T = T - T_0$.

4.2 Linear temperature rise (LTR)

For a FG nanobeam for which the beam thickness is thin enough, the temperature distribution is assumed to be varied linearly through the thickness as follows

$$T = T_m + \Delta T\left(\frac{z}{h} + \frac{1}{2}\right), \tag{46}$$

where the buckling temperature difference is $\Delta T = T_c - T_m$ in which T_c and T_m are the temperature of the top surface which is ceramic-rich and the bottom surface which is metal-rich, respectively.

4.3 Nonlinear temperature rise (NLTR)

The one-dimensional temperature distribution through-the-thickness can be obtained by solving the steady-state heat conduction equation with the boundary conditions on bottom and top surfaces of the beam across the thickness

$$-\frac{\mathrm{d}}{\mathrm{d}z}\left(\kappa(z,T)\frac{\mathrm{d}T}{\mathrm{d}z}\right) = 0, \quad T|_{z=h/2} = T_c, \quad T|_{z=-h/2} = T_m \tag{47}$$

The solution of above equation is

$$T = T_m + (T_c - T_m)\frac{\int_{-h/2}^{z} \frac{1}{\kappa(z,T)}\mathrm{d}z}{\int_{-h/2}^{h/2} \frac{1}{\kappa(z,T)}\mathrm{d}z}. \tag{48}$$

5. Numerical results and discussions

The thermal vibration analysis of FG nanobeams are investigated using the Navier method based upon third order shear deformation theory and nonlocal elasticity theory. The effective material properties, that elasticity modulus and mass density of the FG nanobeam vary through the thickness direction according to power law distribution. Simply supported boundary condition is

Table 2 Comparison of the non-dimensional fundamental frequency for a FG nanobeam with various power-law indexes at $L/h = 20$ and $\Delta T = 0$ K

	$p = 0$			$p = 0.5$		
μ	EBT (Eltaher *et al.* 2012)	TBT (Rahmani and Pedram (24))	Present RBT	EBT (Eltaher *et al.* 2012)	TBT (Rahmani and Pedram (24))	Present RBT
0	9.8797	9.8296	9.82957	7.8061	7.7149	7.71546
1	9.4238	9.3777	9.377686	7.4458	7.3602	7.36078
2	9.0257	8.9829	8.982894	7.1312	7.0504	7.0509
3	8.6741	8.6341	8.634103	6.8533	6.7766	6.77714
4	8.3607	8.323	8.323021	6.6057	6.5325	6.53296
5	8.0789	8.0433	8.043309	6.383	6.3129	6.31342
	$p = 1$			$p = 5$		
μ	EBT (Eltaher *et al.* 2012)	TBT (Rahmani and Pedram (24))	Present RBT	EBT (Eltaher *et al.* 2012)	TBT (Rahmani and Pedram (24))	Present RBT
0	7.0904	6.9676	6.967613	6.0025	5.9172	5.916152
1	6.7631	6.6473	6.6473	5.7256	5.6452	5.644175
2	6.4774	6.3674	6.367454	5.4837	5.4075	5.406561
3	6.2251	6.1202	6.120217	5.2702	5.1975	5.196632
4	6.0001	5.8997	5.899708	5.0797	5.0103	5.0094
5	5.7979	5.7014	5.701436	4.9086	4.8419	4.841049

considered for which required the Navier method. The effects of FG material graduation, nonlocality effect, slenderness ratio and thermal load on the non-dimensional natural frequencies of the FG nanobeam will be figured out. FG nanobeam is composed of steel (SUS304) and alumina (Al_2O_3) where its properties are given in Table 1. The bottom surface of the beam is pure Steel, whereas the top surface of the beam is pure Alumina. The beam geometry has the following dimensions: L (length)=10000 nm, b (width)=1000 nm. A 5K increase in metal surface to reference temperature T_0 of FG nanobeam is considered, i.e., $T_m - T_0 = 5K$. The following dimensionless relation is defined in order to calculate the non-dimensional natural frequencies

$$\widehat{\omega} = \omega_n L^2 \sqrt{\frac{\rho_c A}{E_c I}}, \tag{49}$$

where $I = bh^3/12$ is the moment of inertia of the cross section of the nanobeam. For the verification purpose, the non-dimensional natural frequency of simply supported FG nanobeam with various nonlocal parameters and power-law exponents are compared with the results presented by Eltaher *et al.* (2012) For Euler-Bernoulli FG nanobeams and Rahmani and Pedram (2014) which has been obtained by analytical method for FG Timoshenko nanobeam. In these works, the material properties are selected as: $E_m = 210$ GPa, $E_c = 390$ GPa, $\rho_m = 7800\ kg/m^3$, $\rho_c = 3900\ kg/m^3$, $\nu_m = 0.3$ and $\nu_c = 0.24$.

The reliability of the presented method and procedure for FG nanobeam may be concluded from Table 2; where the results are in an excellent agreement as values of non-dimensional

Table 3 The variation of the first non-dimensional fundamental frequency for a FG nanobeam with various power-law indexes and nonlocal parameters ($L/h = 20$)

μ		$\Delta T = 10$ K				$\Delta T = 30$ K				$\Delta T = 60$ K			
		Power-law index				Power-law index				Power-law index			
		0.2	0.5	1	5	0.2	0.5	1	5	0.2	0.5	1	5
	UTR	7.79277	6.59689	5.76592	4.68775	7.42151	6.23435	5.41109	4.34763	6.80468	5.62434	4.8070	3.75680
0	LTR	7.79580	6.60104	5.76989	4.68953	7.61805	6.43025	5.60278	4.52550	7.33302	6.15462	5.3315	4.25646
	NLTR	7.79717	6.60334	5.77265	4.69140	7.62269	6.43802	5.61216	4.53189	7.34417	6.17329	5.35413	4.27204
	UTR	7.41773	6.27724	5.48484	4.45696	7.02655	5.89484	5.11022	4.09737	6.37147	5.24525	4.46528	3.46369
1	LTR	7.42088	6.28154	5.48893	4.45874	7.23381	6.10160	5.31273	4.28556	6.93289	5.81020	5.02555	4.00010
	NLTR	7.42232	6.28395	5.49184	4.46071	7.23870	6.10979	5.61216	4.29230	6.94468	5.82998	5.04954	4.01667
	UTR	7.08933	5.99724	5.23855	4.25463	6.67884	5.59554	4.84466	3.87599	5.98569	4.90625	4.15844	3.19838
2	LTR	7.09260	6.00169	5.24276	4.25641	6.89652	5.81291	5.05775	4.07436	6.58009	5.50608	4.75497	3.77267
	NLTR	7.09411	6.00421	5.24581	4.25848	6.90165	5.82151	5.06814	4.08145	6.59252	5.52695	4.78032	3.79023
	UTR	6.79854	5.74922	5.02032	4.07526	6.36922	5.32867	4.60757	3.67791	5.63803	4.59936	3.87936	2.95488
3	LTR	6.80192	5.75381	5.02465	4.07705	6.59711	5.55646	4.83109	3.88635	6.2655	5.23446	4.51291	3.56854
	NLTR	6.80349	5.75644	5.02783	4.07920	6.60248	5.56545	4.84196	3.89378	6.27854	5.25640	4.53962	3.58711
	UTR	6.53859	5.52742	4.82510	3.91472	6.09089	5.08841	4.39384	3.49893	5.32148	4.31853	3.62267	2.72856
4	LTR	6.54208	5.53216	4.82956	3.91652	6.32879	5.32645	4.62765	3.71736	5.98224	4.98949	4.29424	3.38349
	NLTR	6.54371	5.53490	4.83286	3.91876	6.33438	5.33583	4.63900	3.72514	5.99590	5.01250	4.32230	3.40307

frequency are consistent with presented analytical solution. It can be observed from Table 2 that the results of nonlocal Reddy beam theory are smaller than those of nonlocal Euler beam theory. This is due to the fact that Euler-Bernoulli beam model cannot capture shear deformation effect.

The variations of the first three non-dimensional frequencies of the simply supported FG nanobeams for various values of power-law exponent ($p = 0.2, 0.5, 1, 5$), nonlocal parameters ($\mu = 0, 1, 2, 3, 4\ \mathrm{nm}^2$) and temperature changes ($\Delta T = 10, 30, 60$ K) for three types of thermal loading at $L/h = 20$ are presented in Tables 3-5. It is seen from the results of these tables that in all cases of thermal loading increasing nonlocal scale parameter leads to decreasing in the non-dimensional frequencies at a constant power-law exponent. So it is worth noting that nonlocal parameter has a remarkable effect on the natural frequencies of FG nanobeams. Also, it is observed that, by fixing nonlocal parameter and increasing power-law exponent the non-dimensional frequencies reduces, especially for lower values of power-law exponent. In addition, it is concluded that the values of non-dimensional frequencies temperature in the case of nonlinear temperature change are bigger than those of uniform and linear temperature change at a constant power-law exponent and slenderness ratio.

The dimensionless frequencies of FG nanobeam versus the power-law exponent under uniform, linear and non-linear temperature rise through-the-thickness at $L/h = 20$ are depicted in Figs. 2-4, respectively. In these figures, regardless of the thermal loading types, the dimensionless natural frequency decreases suddenly as the power-law exponent increases from 0 to 2, then decreases monotonically as the power-law exponent increases from 2 to 10. It can be observed from the results of the figures that by increasing the nonlocal parameter the first dimensionless frequency reduce for every power-law exponent and temperature change, which indicates the notability of the nonlocal effect.

Table 4 The variation of the second non-dimensional fundamental frequency for a FG nanobeam with various power-law indexes and nonlocal parameters ($L/h = 20$)

μ		$\Delta T = 10$ K				$\Delta T = 30$ K				$\Delta T = 60$ K			
		Power-law index				Power-law index				Power-law index			
		0.2	0.5	1	5	0.2	0.5	1	5	0.2	0.5	1	5
	UTR	31.3181	26.5766	23.2771	18.9794	30.9614	26.2332	22.9447	18.6650	30.3966	25.6860	22.4123	18.1579
0	LTR	31.3221	26.5825	23.2834	18.9840	31.1513	26.4218	23.1287	18.8346	30.8815	26.1654	22.8799	18.5923
	NLTR	31.3235	26.5847	23.2861	18.9858	31.1558	26.4293	23.1377	18.8407	30.8921	26.1829	22.9009	18.6065
	UTR	26.4591	22.4459	19.6535	16.0172	26.0342	22.0352	19.2548	15.6386	25.3583	21.3778	18.6132	15.0249
1	LTR	26.4634	22.4521	19.6599	16.0213	26.2594	22.2588	19.4728	15.8396	25.9373	21.9512	19.1732	15.5467
	NLTR	26.4650	22.4548	19.6631	16.0235	26.2648	22.2677	19.4835	15.8469	25.9499	21.9720	19.1982	15.5637
	UTR	23.3068	19.7652	17.3013	14.0933	22.8222	19.2956	16.8444	13.6585	22.0469	18.5394	16.1045	12.9483
2	LTR	23.3114	19.7717	17.3078	14.0972	23.0786	19.5502	17.0927	13.8876	22.7105	19.1976	16.7484	13.5500
	NLTR	23.3133	19.7748	17.3115	14.0997	23.0847	19.5603	17.1049	13.8959	22.7248	19.2214	16.7771	13.5695
	UTR	21.0485	17.8441	15.6150	12.7134	20.5098	17.3211	15.1054	12.2275	19.6427	16.4731	14.2739	11.4265
3	LTR	21.0534	17.8509	15.6218	12.7172	20.7946	17.604	15.3814	12.4825	20.3846	17.2104	14.9964	12.1038
	NLTR	21.0554	17.8543	15.6258	12.7199	20.8013	17.6153	15.3950	12.4917	20.4005	17.2369	15.0284	12.1257
	UTR	19.3271	16.3792	14.3288	11.6604	18.7383	15.8068	13.7703	11.1270	17.7845	14.8716	12.8513	10.2385
4	LTR	19.3322	16.3864	14.3358	11.6641	19.0495	16.116	14.0723	11.4062	18.6006	15.6842	13.6491	10.9892
	NLTR	19.3344	16.3901	14.3402	11.6671	19.0569	16.1284	14.0871	11.4163	18.618	15.7134	13.6843	11.0132

Table 5 The variation of the third non-dimensional fundamental frequency for a FG nanobeam with various power-law indexes and nonlocal parameters ($L/h = 20$)

μ		$\Delta T = 10$ K				$\Delta T = 30$ K				$\Delta T = 60$ K			
		Power-law index				Power-law index				Power-law index			
		0.2	0.5	1	5	0.2	0.5	1	5	0.2	0.5	1	5
	UTR	69.3337	58.8561	51.5575	42.0176	68.9817	58.5225	51.2382	41.7188	68.4255	57.9895	50.7237	41.2323
0	LTR	69.3394	58.8650	51.5677	42.0268	69.1733	58.7134	51.4250	41.8919	68.9083	58.4661	51.1881	41.6637
	NLTR	69.3408	58.8673	51.5704	42.0287	69.1778	58.7209	51.4341	41.8980	68.9188	58.4835	51.209	41.6779
	UTR	50.3412	42.7196	37.4109	30.4734	49.8482	42.2460	36.9530	30.0400	49.0685	41.4919	36.2199	29.3410
1	LTR	50.3471	42.7283	37.4203	30.4807	50.1114	42.5074	37.2082	30.2759	49.7388	42.1542	36.8659	29.9424
	NLTR	50.349	42.7315	37.4241	30.4832	50.1177	42.5178	37.2207	30.2844	49.7533	42.1784	36.8949	29.9621
	UTR	41.4201	35.1373	30.7616	25.0445	40.8162	34.5543	30.1957	24.5064	39.8571	33.6226	29.2868	23.6357
2	LTR	41.4264	35.1464	30.7711	25.0509	41.1366	34.8723	30.5060	24.7933	40.6791	34.4360	30.0812	24.3773
	NLTR	41.4287	35.1502	30.7757	25.0540	41.1442	34.8850	30.5212	24.8036	40.6969	34.4656	30.1168	24.4015
	UTR	35.9699	30.5035	26.6968	21.7240	35.2709	29.8267	26.0383	21.0961	34.1546	28.7388	24.9741	20.0727
3	LTR	35.9766	30.5131	26.7065	21.7299	35.6409	30.1939	26.3966	21.4276	35.1102	29.6860	25.9008	20.9404
	NLTR	35.9793	30.5175	26.7117	21.7335	35.6496	30.2086	26.4142	21.4396	35.1308	29.7204	25.9421	20.9685
	UTR	32.1966	27.2943	23.8807	19.4224	31.4125	26.5334	23.1393	18.7139	30.1523	25.3021	21.9318	17.5483
4	LTR	32.2038	27.3044	23.8907	19.4281	31.8270	26.9451	23.5411	19.0860	31.2305	26.3728	22.9812	18.5343
	NLTR	32.2067	27.3093	23.8966	19.4321	31.8369	26.9615	23.5609	19.0994	31.2537	26.4114	23.0277	18.5661

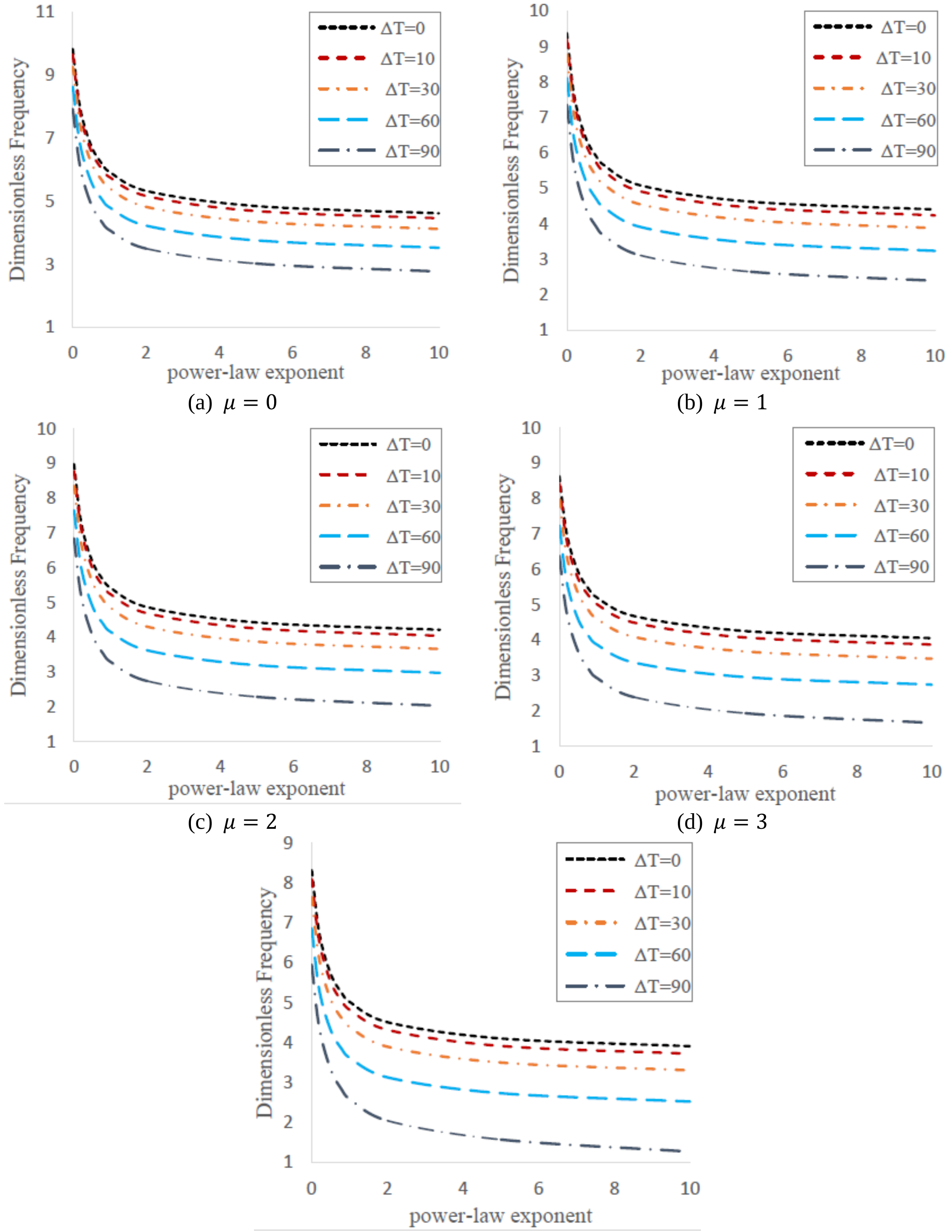

(e) $\mu = 4$

Fig. 2 The variation of the first dimensionless frequency of the FG nanobeam under uniform temperature change with power-law exponent and temperature rises for different nonlocal parameters ($L/h = 20$)

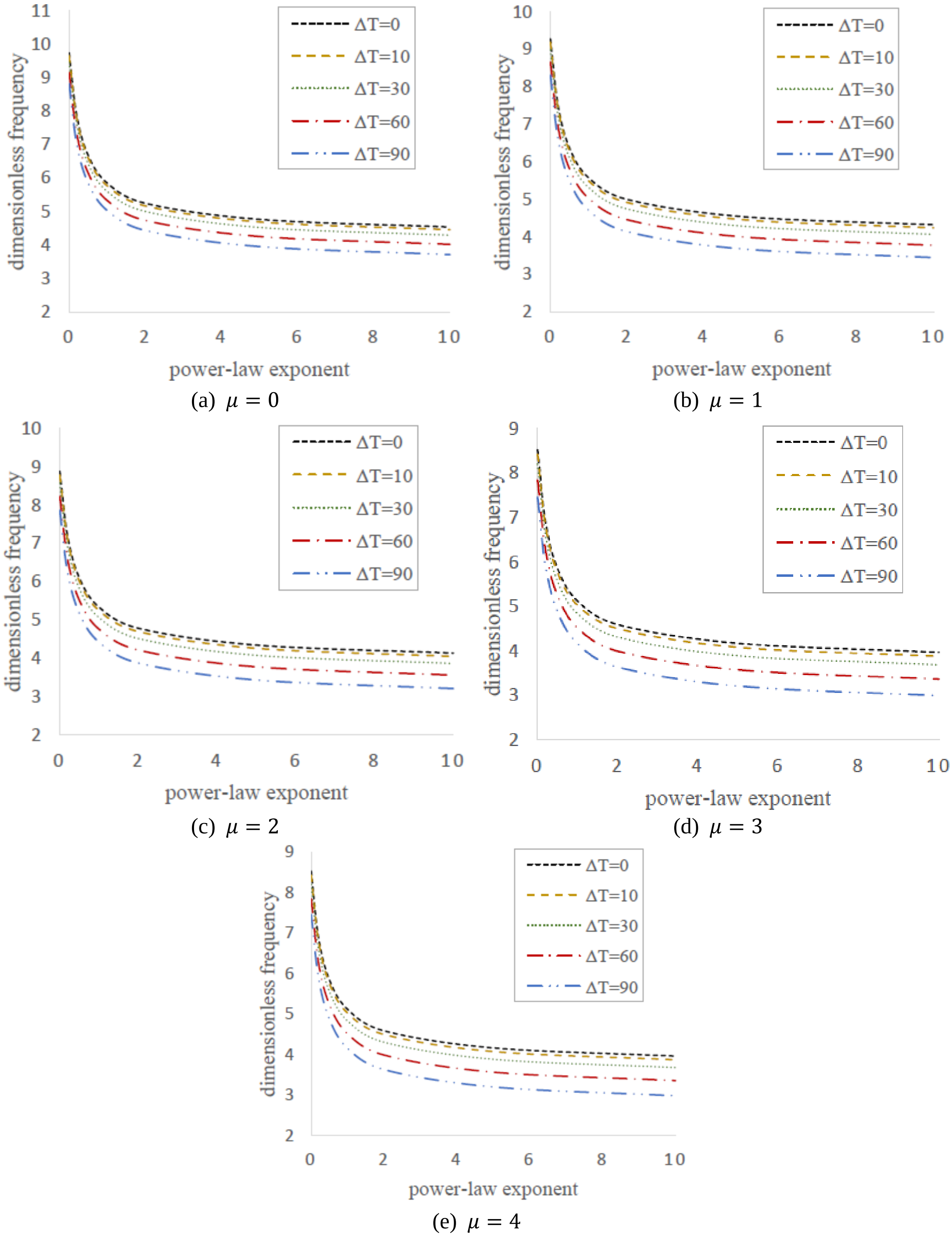

Fig. 3 The variation of the first dimensionless frequency of the FG nanobeam under linear temperature change with power-law exponent and temperature rises for different nonlocal parameters ($L/h = 20$)

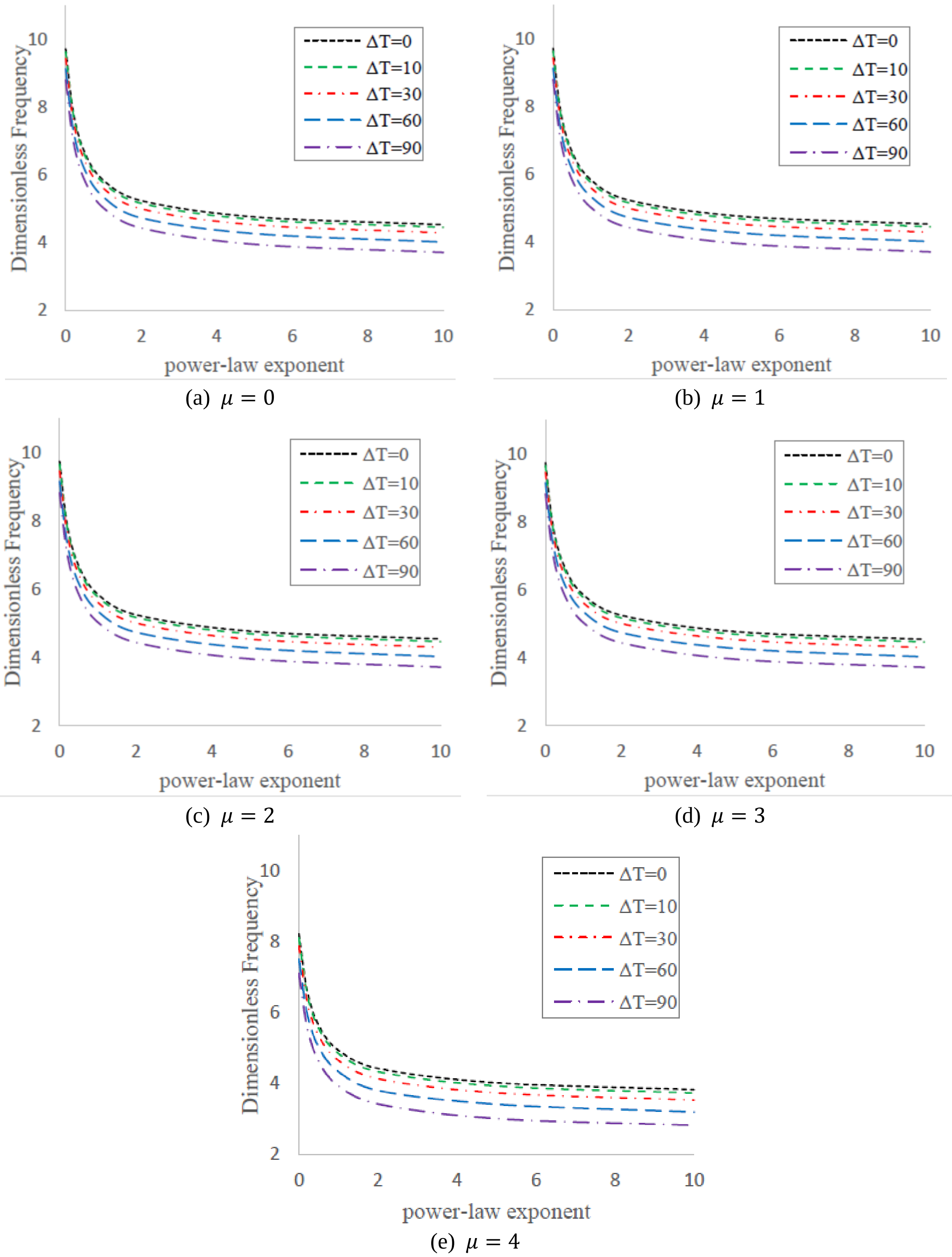

(a) $\mu = 0$ (b) $\mu = 1$ (c) $\mu = 2$ (d) $\mu = 3$ (e) $\mu = 4$

Fig. 4 The variation of the first dimensionless frequency of FG nanobeam under non-linear temperature change for different nonlocal parameters $(L/h = 20)$

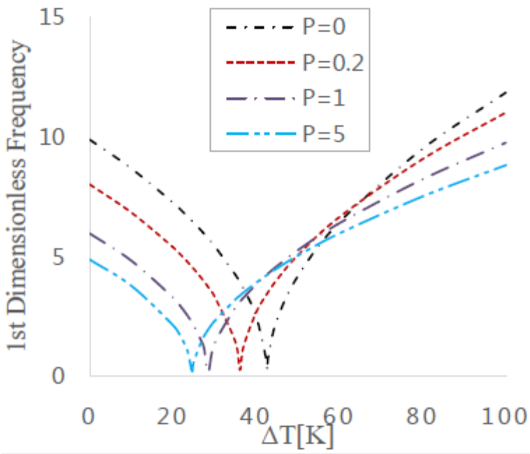

(a) $\mu = 0$

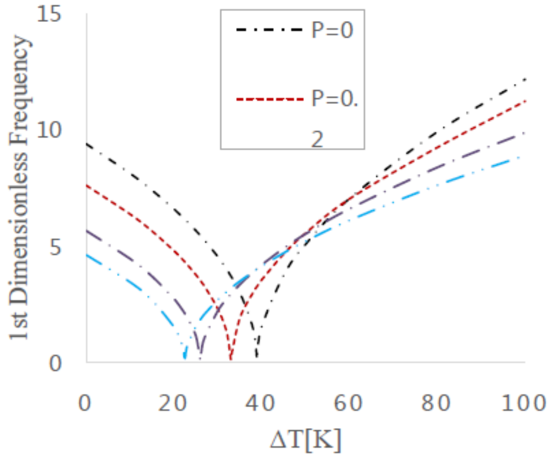

(b) $\mu = 1$

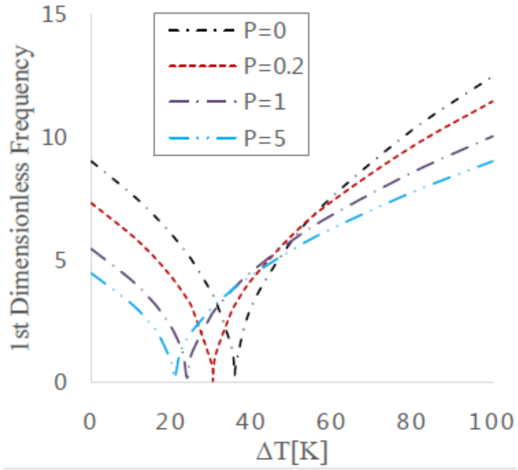

(c) $\mu = 2$

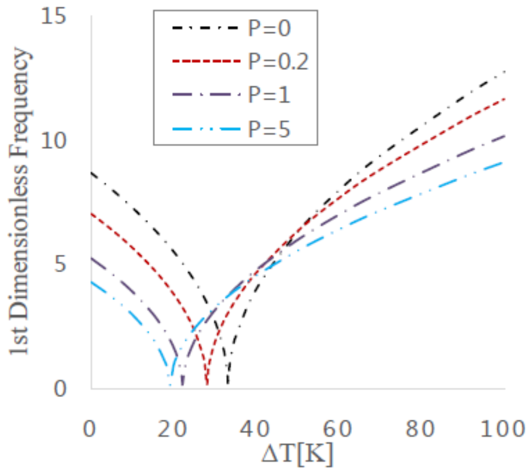

(d) $\mu = 3$

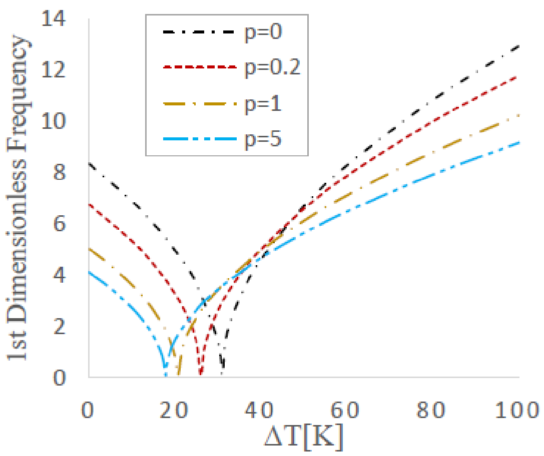

(e) $\mu = 4$

Fig. 5 Variations of the first dimensionless natural frequency of the FG nanobeam with respect to uniform temperature change for different values of power-law exponent and nonlocal parameters ($L/h = 20$)

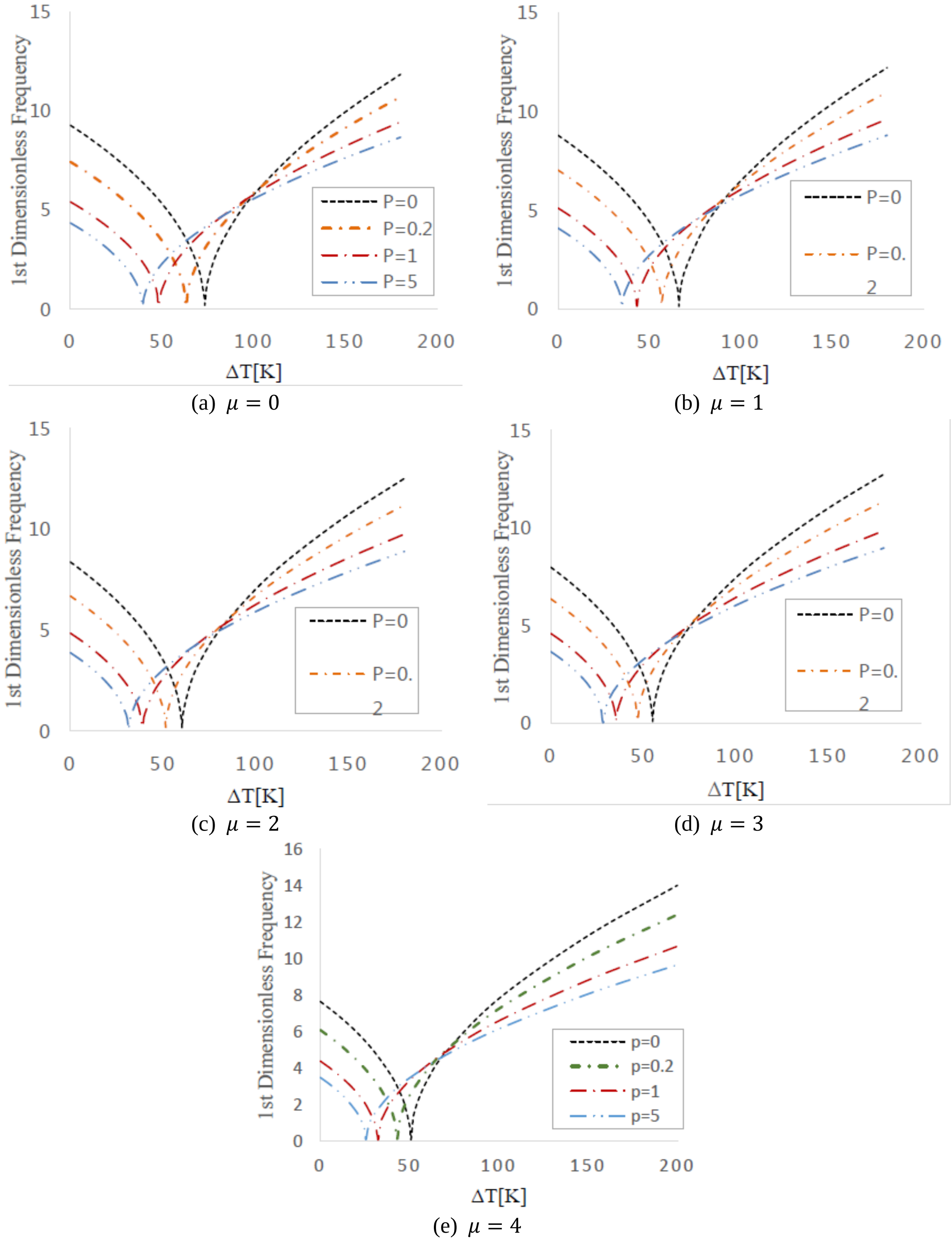

Fig. 6 Variations of the first dimensionless natural frequency of the FG nanobeam with respect to linear temperature change for different values of power-law exponent and nonlocal parameters ($L/h = 25$)

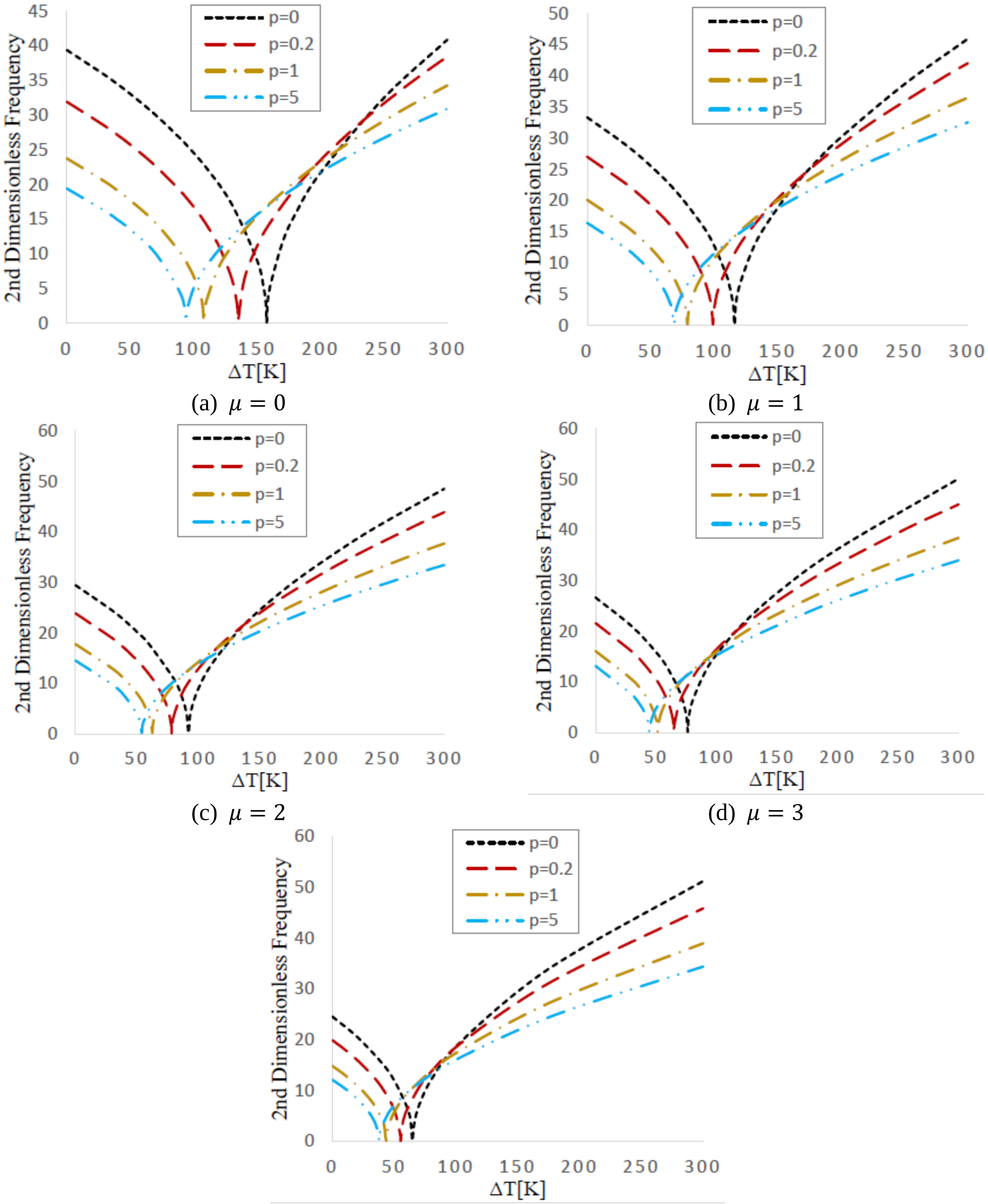

(a) $\mu = 0$ (b) $\mu = 1$

(c) $\mu = 2$ (d) $\mu = 3$

(e) $\mu = 4$

Fig. 7 Variations of the first dimensionless natural frequency of the FG nanobeam with respect to non-linear temperature change for different values of power-law exponent and nonlocal parameters ($L/h = 50$)

Also, it must be noted that the dimensionless natural frequency of the FG nanobeam under nonlinear temperature rise is greater than that of the FG nanobeam under linear temperature rise and the latter is greater than that of the FG nanobeam under uniform temperature rise. Figs. 5-7 illustrate the variation of first dimensionless natural frequency with changing of the power-law exponent for different nonlocal parameter at slenderness ratio $L/h = 50$ of FG nanobeam under uniform, linear and non-linear temperature change, respectively.

Also the variation of second dimensionless natural frequency with temperature rise for different power-law exponents and nonlocal parameters at slenderness ratio $L/h = 50$ in the case of uniform, linear and non-linear temperature change, are demonstrated in Figs. 8-10, respectively. Also, the variation of third dimensionless natural frequency with temperature rise with above mentioned conditions is presented in Figs. 11-13. It is seen that before a prescribed temperature, i.e., the critical buckling temperature, as temperature increases the first dimensionless frequency reduces. This is associated to the reduction in total stiffness of the beam, since geometrical stiffness of FG nanobeam diminishes as temperature rises. Near the critical buckling temperature, dimensionless frequency trends to zero. It is observed that temperature dependency of the material constituents leads to more accurate conclusions, whereas with supposing temperature independent material properties, critical buckling temperature point is exaggerated. Moreover, in the pre-buckling region, with the temperature dependent assumption, predicted frequencies are smaller than those frequencies obtained with the assumption of temperature independent material. This is due to the less Young's modulus of the material constituents in the case of temperature dependent material. Also, it should be stated that, by increasing the nonlocal parameter the critical temperature point shifts to the left.

Figs. 14-16 show the variations of the first dimensionless natural frequency of the S-S FG nanobeam under uniform, linear and non-linear temperature change with respect to temperature change, respectively for different values of nonlocal parameters and power-law indexes ($L/h = 50$). It should be noted that compressive axial forces as resultants of thermal stresses arising from the temperature rise in beams with micro/nano scales, can lead to buckling the beams if its value passes the critical value. By imposing a high external pressure to the FG nanobeam structure, the high stresses induced in the structure will influence its integrity and the structure is talented and disposed to failure. Therefore, it is observed from these figures that dimensionless frequencies of the FG nanobeam approaches to zero around a prescribed temperature which is the critical buckling temperature. Before the critical buckling point, as temperature rises the dimensionless frequency reduces, but after that point, as temperature growths the dimensionless frequency increases. Moreover, in the pre-buckling domain, by increasing the nonlocal parameter, the dimensionless natural frequency diminishes at a constant power-law exponent, while in the post-buckling domain, as the nonlocal parameter increases the dimensionless frequency raises. Another notable observation is that, the critical point is postponed with the assumption of the smaller power-law indexes, related to the fact that the lower power-law indexes result in the increase of stiffness of the beam.

The variations of the first dimensionless natural frequency of the S-S FG nanobeam under uniform, linear and non-linear temperature rise with respect to temperature change for different values of slenderness ratios ($L/h = 40, 50, 60$) and nonlocal parameters at $p = 0.2$ is presented in Figs. 17-19, respectively. It is revealed that for S-S FG nanobeams in the pre-buckling domain, increasing slenderness ratio leads to decrease in natural frequency. But in the post-buckling domain increase of slenderness ratio leads to increment in natural frequency. Also, it is seen that when nonlocal parameter increases the critical buckling point continuously moves to the left at a fixed material power-law index.

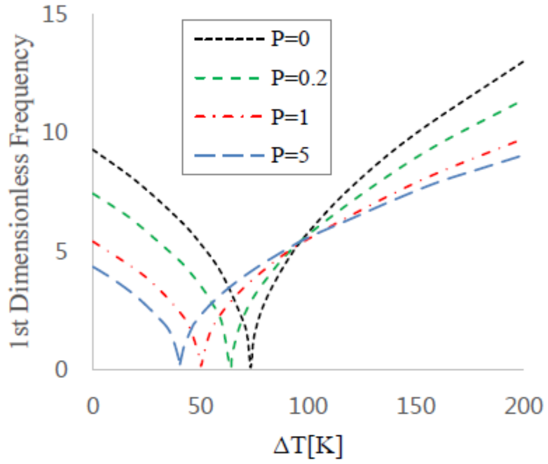

(a) $\mu = 0$

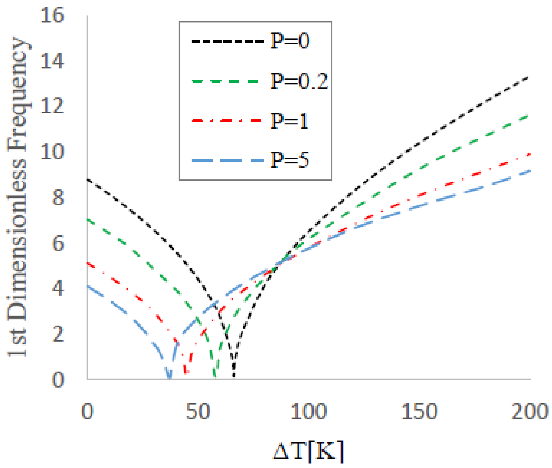

(b) $\mu = 1$

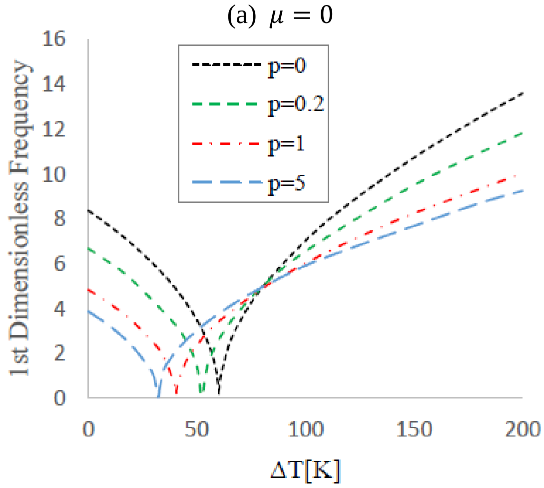

(c) $\mu = 2$

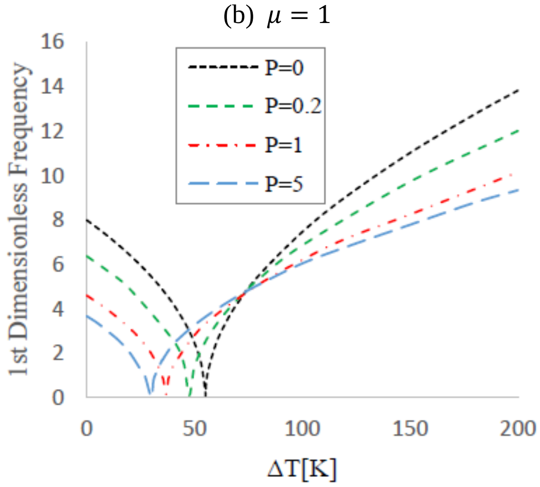

(d) $\mu = 3$

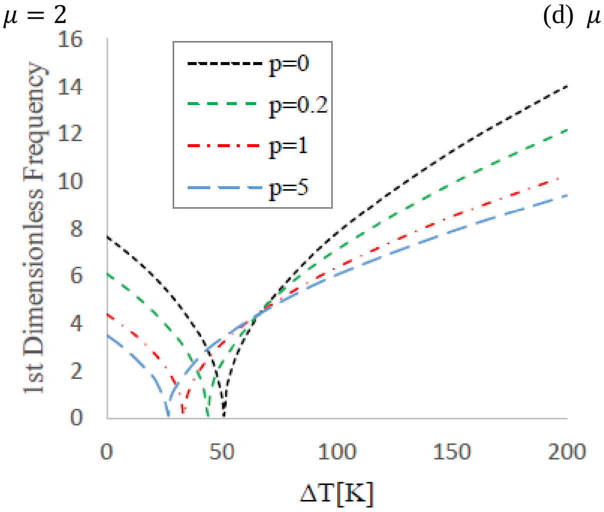

(e) $\mu = 4$

Fig. 8 Variations of the second dimensionless natural frequency of the FG nanobeam with respect to uniform temperature change for different values of power-law exponents and nonlocal parameters ($L/h = 50$)

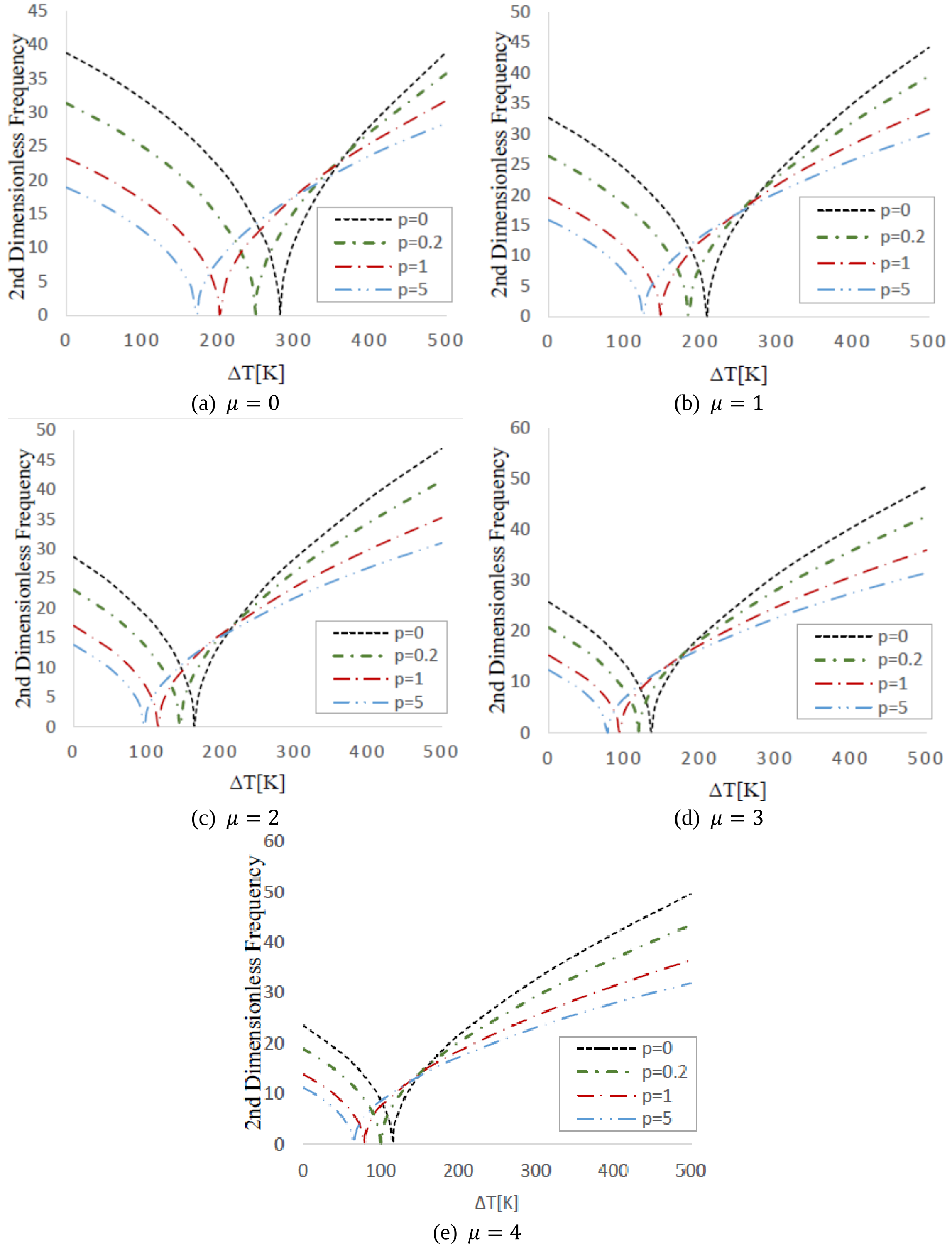

Fig. 9 Variations of the second dimensionless natural frequency of the FG nanobeam with respect to linear temperature change for different values of power-law exponents and nonlocal parameters ($L/h = 50$)

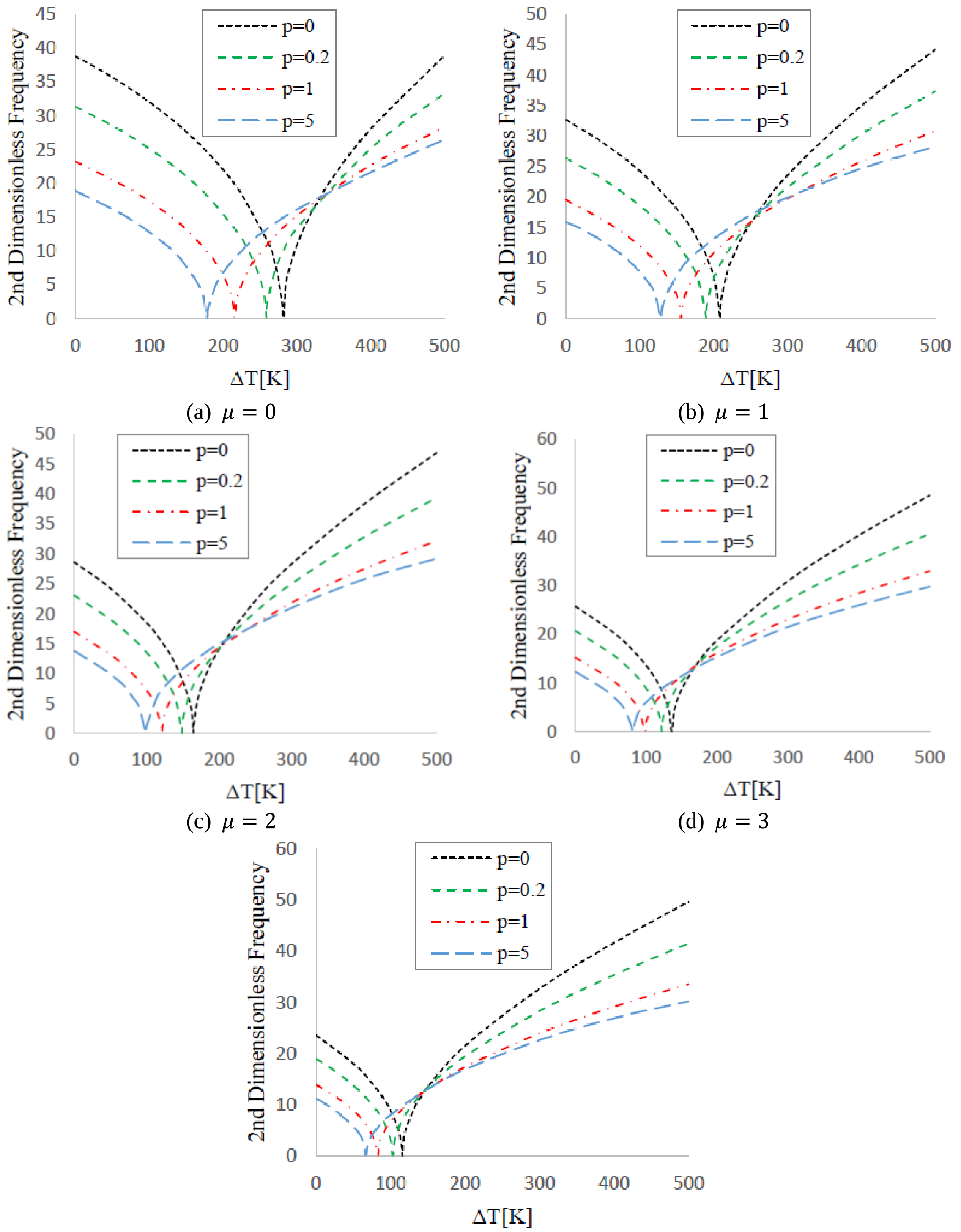

(a) $\mu = 0$ (b) $\mu = 1$

(c) $\mu = 2$ (d) $\mu = 3$

(e) $\mu = 4$

Fig. 10 Variations of the second dimensionless natural frequency of the FG nanobeam with respect to non-linear temperature change for different values of power-law exponents and nonlocal parameters ($L/h = 50$)

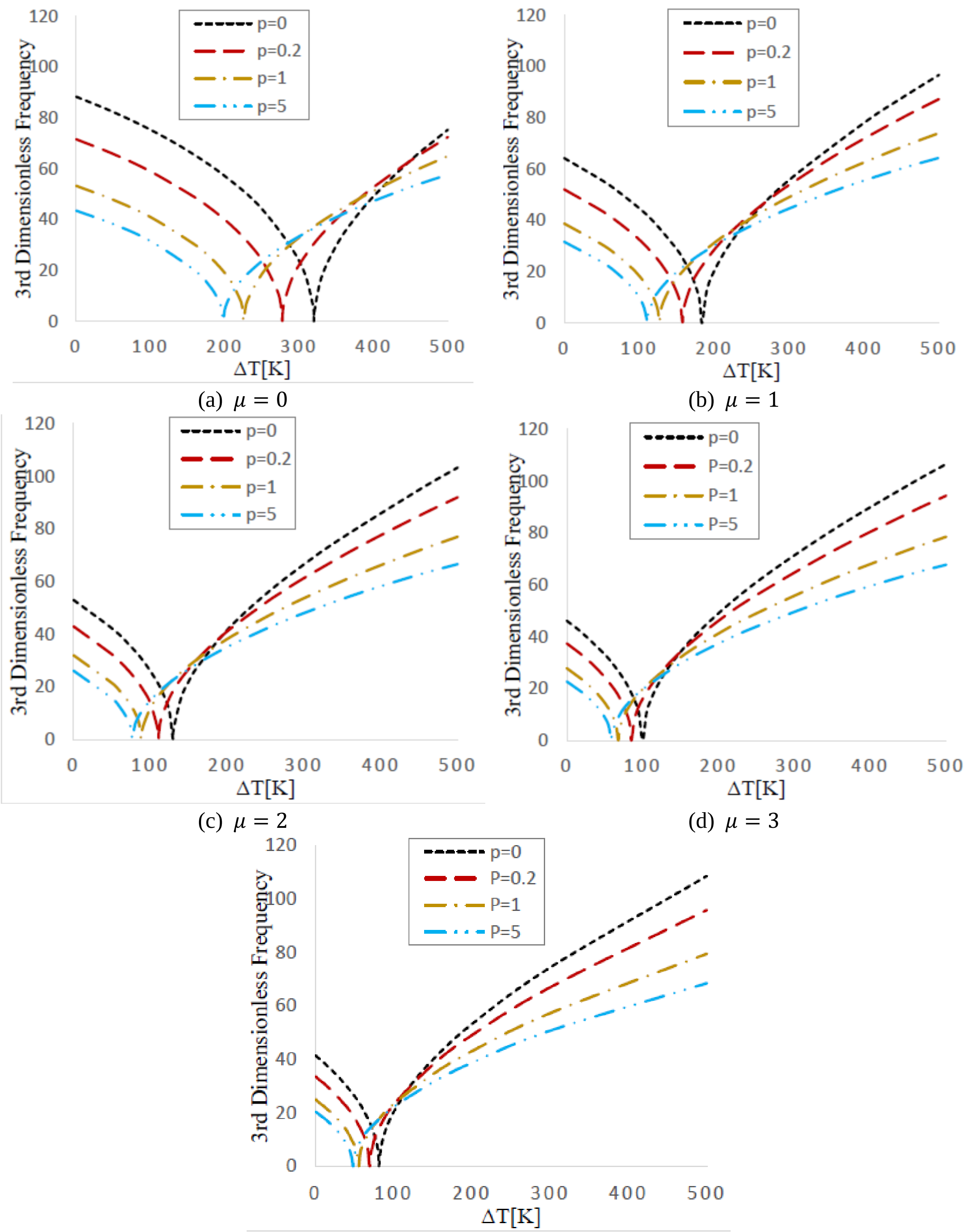

(a) $\mu = 0$ (b) $\mu = 1$

(c) $\mu = 2$ (d) $\mu = 3$

(e) $\mu = 4$

Fig. 11 Variations of the third dimensionless natural frequency of the FG nanobeam with respect to uniform temperature change for different values of gradient indexes and nonlocal parameters ($L/h = 50$)

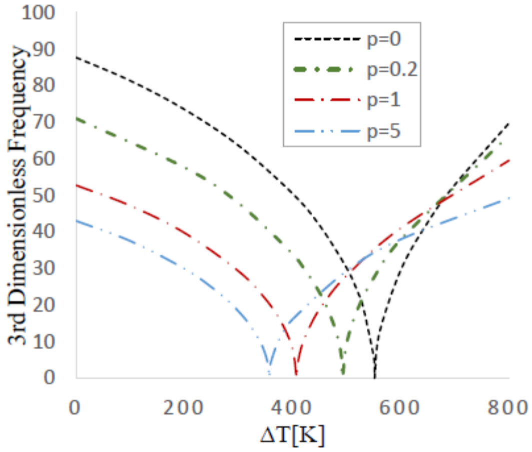

(a) $\mu = 0$

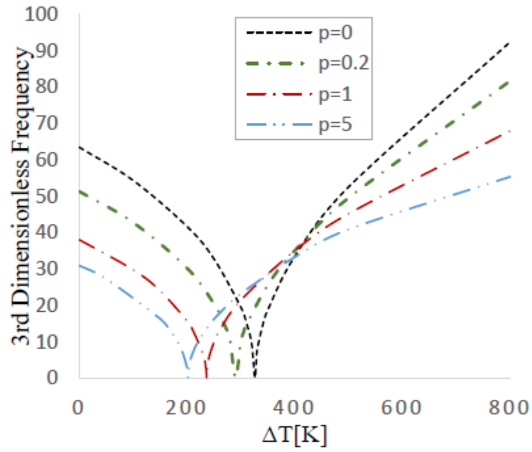

(b) $\mu = 1$

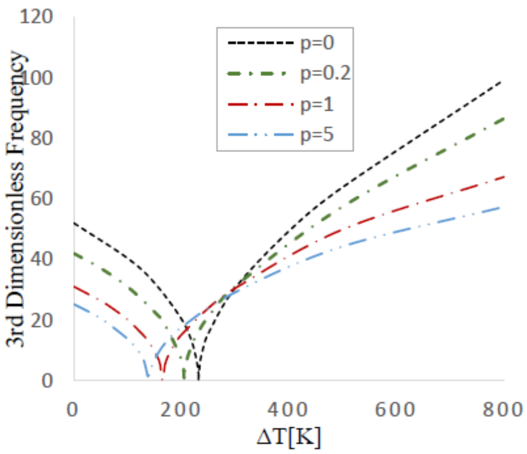

(c) $\mu = 2$

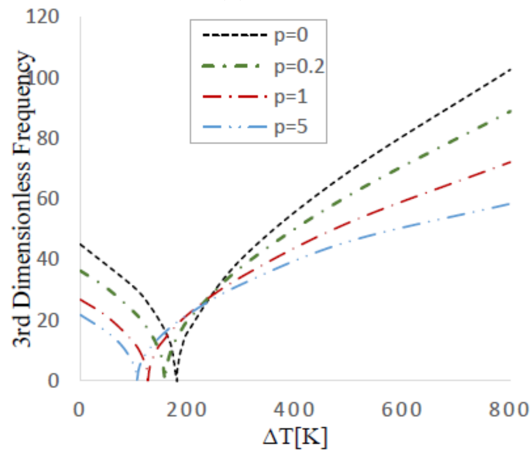

(d) $\mu = 3$

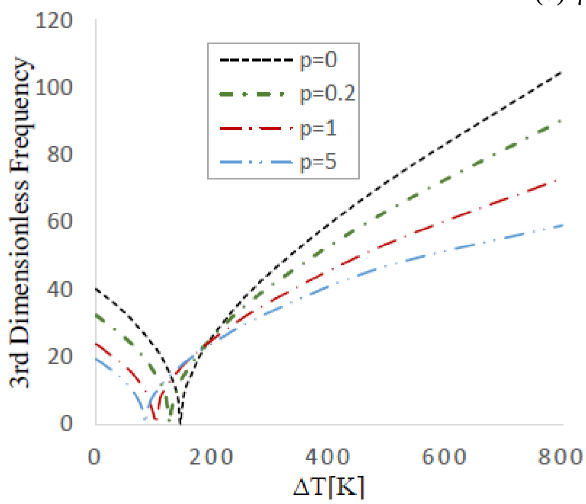

(e) $\mu = 4$

Fig. 12 Variations of the third dimensionless natural frequency of the FG nanobeam with respect to linear temperature change for different values of gradient indexes and nonlocal parameters $(L/h = 50)$

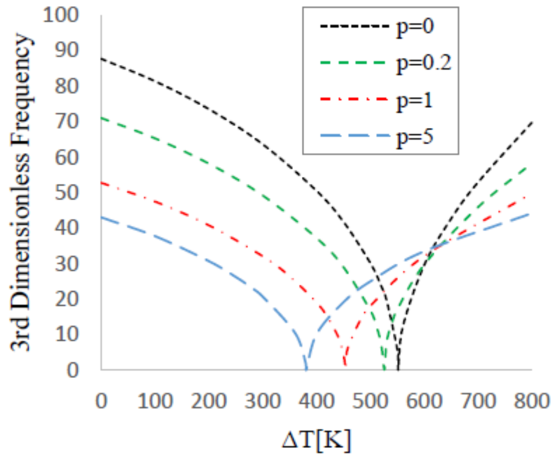

(a) $\mu = 0$

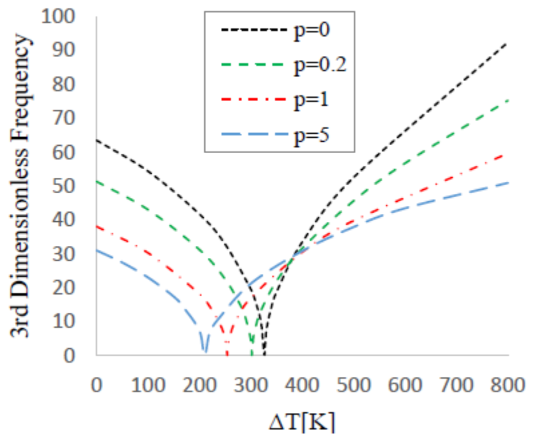

(b) $\mu = 1$

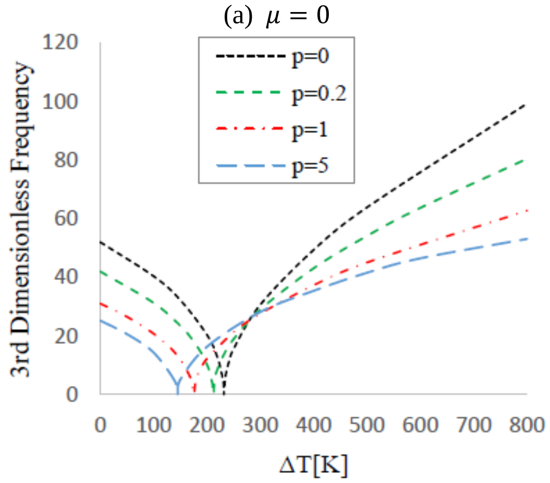

(c) $\mu = 2$

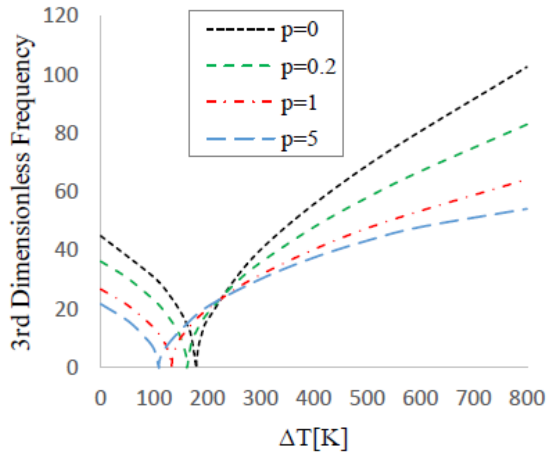

(d) $\mu = 3$

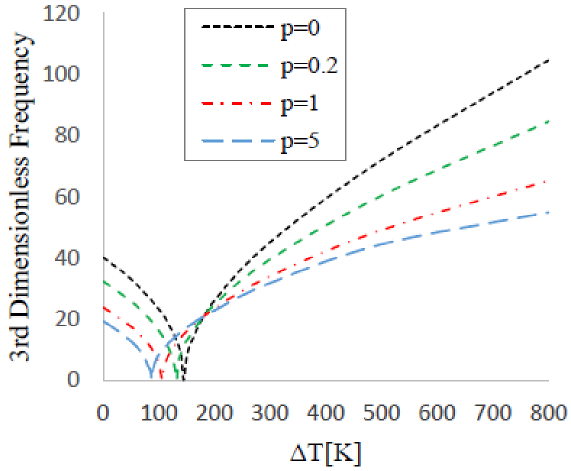

(e) $\mu = 4$

Fig. 13 Variations of the third dimensionless natural frequency of the FG nanobeam with respect to non-linear temperature change for different values of gradient indexes and nonlocal parameters ($L/h = 50$)

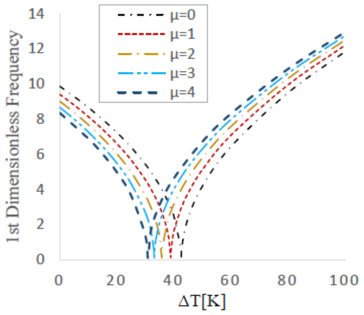

(a) $p = 0$

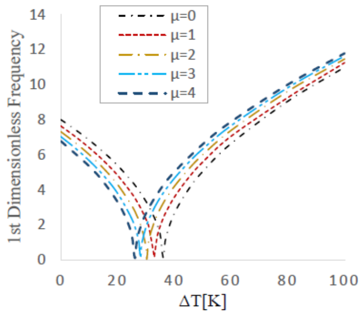

(b) $p = 0.2$

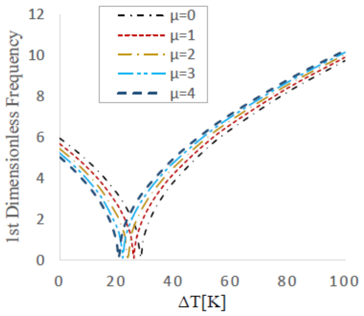

(c) $p = 1$

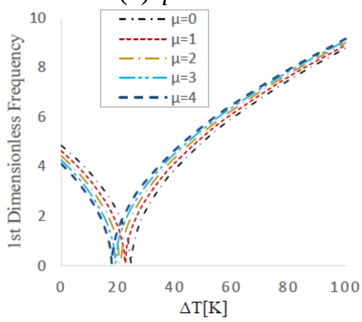

(d) $p = 5$

Fig. 14 Variations of the first dimensionless natural frequency of the FG nanobeam with respect to uniform temperature change for different values of nonlocal parameters and power-law exponents ($L/h = 50$)

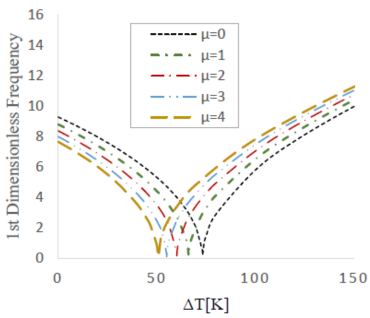

(a) $p = 0$

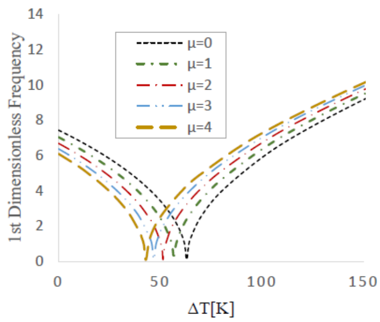

(b) $p = 0.2$

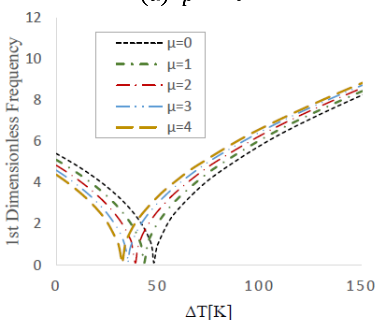

(c) $p = 1$

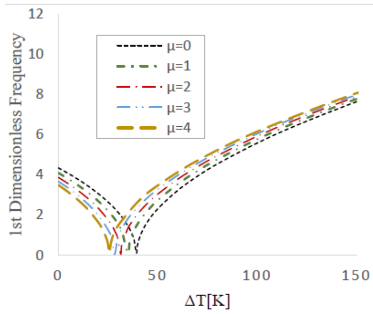

(d) $p = 5$

Fig. 15 Variations of the first dimensionless natural frequency of the FG nanobeam with respect to linear temperature change for different values of nonlocal parameters and power-law exponents ($L/h = 50$)

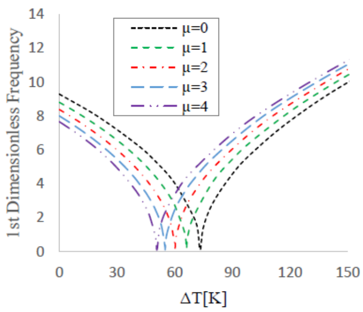

(a) $p = 0$

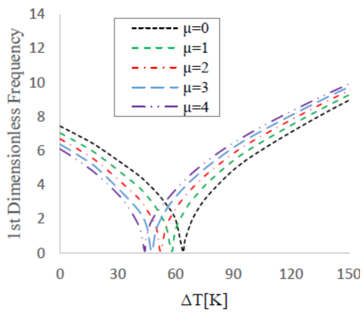

(b) $p = 0.2$

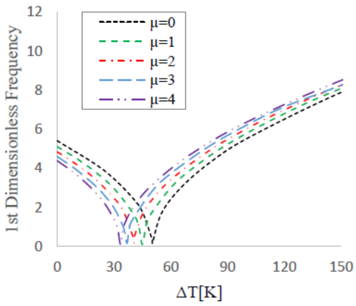

(c) $p = 1$

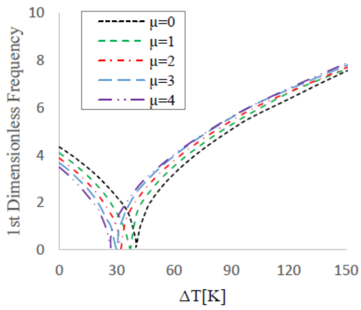

(d) $p = 5$

Fig. 16 Variations of the first dimensionless natural frequency of the FG nanobeam with respect to non-linear temperature change for different values of nonlocal parameters and power-law exponents ($L/h = 50$)

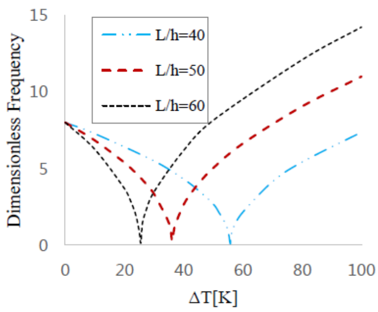

(a) $\mu = 0$

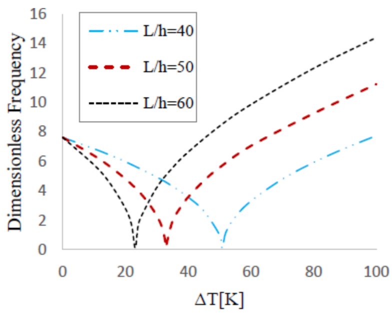

(b) $\mu = 1$

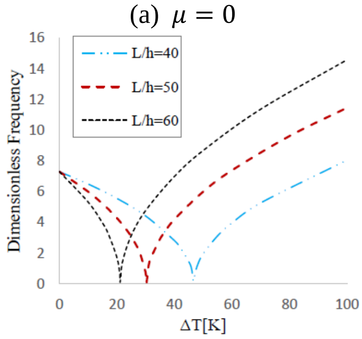

(c) $\mu = 2$

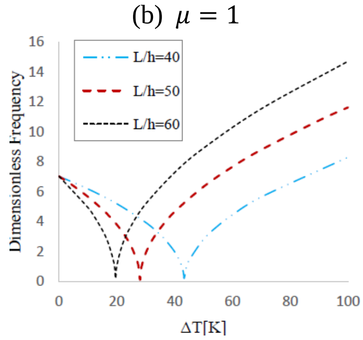

(d) $\mu = 3$

Fig. 17 Variations of the first dimensionless natural frequency of the FG nanobeam with respect to uniform temperature change for different values of slenderness ratios and nonlocal parameters ($p = 0.2$ and $L/h = 50$)

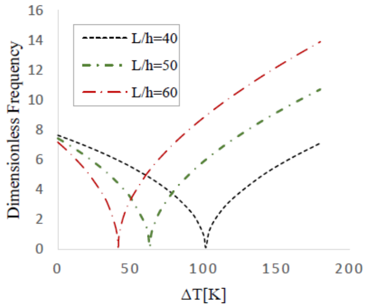

(a) $\mu = 0$

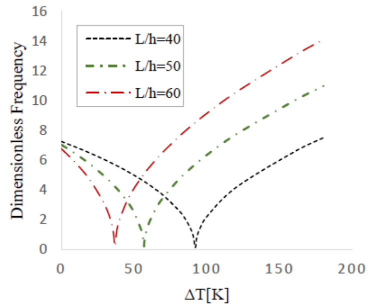

(b) $\mu = 1$

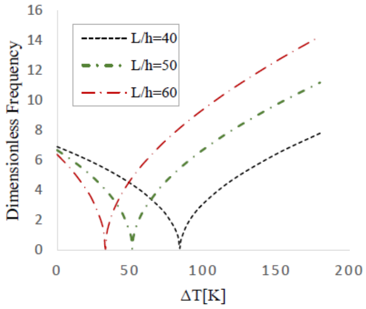

(c) $\mu = 2$

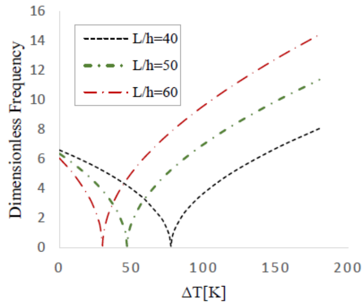

(d) $\mu = 3$

Fig. 18 Variations of the first dimensionless natural frequency of the FG nanobeam with respect to linear temperature change for different values of slenderness ratios and nonlocal parameters ($p = 0.2$ and $L/h = 50$)

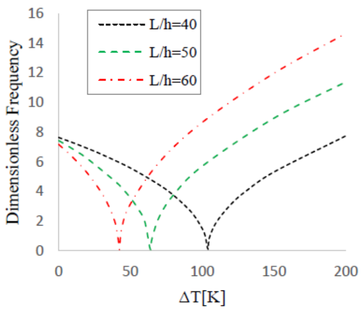

(a) $\mu = 0$

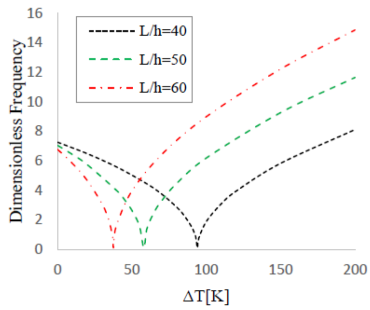

(b) $\mu = 1$

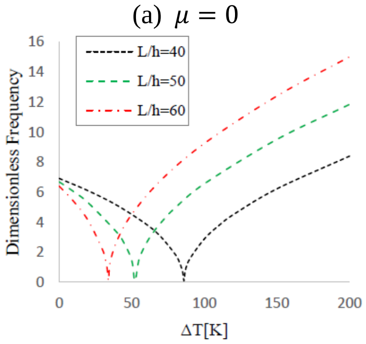

(c) $\mu = 2$

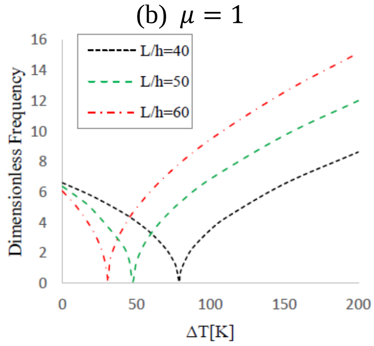

(d) $\mu = 3$

Fig. 19 Variations of the first dimensionless natural frequency of the FG nanobeam with respect to non-linear temperature change for different values of slenderness ratios and nonlocal parameters

6. Conclusions

The thermal vibration analysis of third-order shear deformable simply-supported FG nanobeams is presented and effects of three types of thermal loading namely, uniform, linear and nonlinear temperature rise on vibration behavior of FG nanobeams are investigated. Material properties of FG nanobeam are assumed to change continuously along the thickness according to the power-law form and are assumed to be temperature-dependent. By using the Hamilton's principle the governing equations of motion are derived and Navier's type solution method is used to solve the equations. The obtained results based are compared with those predicted by the previous works to verify the accuracy of the present model. Selected numerical results are presented to indicate the effects of the power-law index, nonlocal parameter, slenderness ratio and thermal load on the vibration characteristics of FG nanobeams. It is observed that the fundamental frequency decreases with the increase in temperature and trends to zero at the critical temperature point. Diminution of frequency with thermal load before the critical point is attributed to the weakening effect of thermally induced compressive stress on the beam stiffness. Moreover, after passing the critical buckling temperature, the fundamental frequency increases with the increment of temperature. Also, it is concluded that under all types of temperature rises, as the power-law exponent growths the natural frequencies diminish, whereas, a reverse trend is observed in the post-buckling domain. In addition it is revealed that for the FG nanobeams subjected to nonlinear temperature changes through the thickness, the obtained frequencies are higher than that for the FG nanobeams subjected to the uniform and linear temperature changes.

References

Adim, B. and Daouadji, T.H. (2016), "Effects of thickness stretching in FGM plates using a quasi-3D higher order shear deformation theory", *Adv. Mater. Res.*, **5**(4), 245-261.

Ansari, R., Gholami, R. and Rouhi, H. (2015), "Size-dependent nonlinear forced vibration analysis of magneto-electro-thermo-elastic Timoshenko nanobeams based upon the nonlocal elasticity theory", *Compos. Struct.*, **126**, 216-226.

Ansari, R., Pourashraf, T. and Gholami, R. (2015), "An exact solution for the nonlinear forced vibration of functionally graded nanobeams in thermal environment based on surface elasticity theory", *Thin-Wall. Struct.*, **93**, 169-176.

Aydogdu, M. (2009), "A general nonlocal beam theory: its application to nanobeam bending, buckling and vibration", *Phys. E.*, **41**(9), 1651-1655.

Civalek, Ö., Demir, Ç. and Akgöz, B. (2010), "Free vibration and bending analyses of cantilever microtubules based on nonlocal continuum model", *Math. Comput. Appl.* **15**(2), 289-298.

Ebrahimi, F. and Jafari, A. (2016), "Buckling behavior of smart MEE-FG porous plate with various boundary conditions based on refined theory", *Adv. Mater. Res.*, **5**(4), 261-276.

Ebrahimi, F., Ehyaei, J. and Babaei, R. (2016), "Thermal buckling of FGM nanoplates subjected to linear and nonlinear varying loads on Pasternak foundation", *Adv. Mater. Res.*, **5**(4), 245-261.

Ebrahimi, F. and Rastgoo, A. (2008a), "Free vibration analysis of smart annular FGM plates integrated with piezoelectric layers", *Smart Mater. Struct.*, **17**(1), 015044.

Ebrahimi, F. and Mohsen, D. (2016), "Dynamic modeling of embedded curved nanobeams incorporating surface effects", *Coupled Syst. Mech.*, **5**(3), 255-267.

Ebrahimi F., Rastgoo, A. and Atai, A.A. (2009a), "Theoretical analysis of smart moderately thick shear deformable annular functionally graded plate", *Eur. J. Mech. A/Sol.*, **28**(5), 962-997.

Ebrahimi, F. and Rastgoo, A. (2008b), "An analytical study on the free vibration of smart circular thin FGM

plate based on classical plate theory", *Thin-Wall. Struct.*, **46**(12), 1402-1408.
Ebrahimi, F. and Rastgoo, A. (2008c), "Free vibration analysis of smart FGM plates", *J. Mech. Syst. Sci. Eng.*, **2**(2), 94-99.
Ebrahimi, F. (2013), "Analytical investigation on vibrations and dynamic response of functionally graded plate integrated with piezoelectric layers in thermal environment", *Mech. Adv. Mater. Struct.*, **20**(10), 854-870.
Ebrahimi, F. and Salari, E. (2015d), "A semi-analytical method for vibrational and buckling analysis of functionally graded nanobeams considering the physical neutral axis position", *Comput. Model. Eng. Sci.*, **105**(2), 151-181.
Ebrahimi, F. and Salari, E. (2015c), "Size-dependent free flexural vibrational behavior of functionally graded nanobeams using semi-analytical differential transform method", *Compos. B*, **79**, 156-169.
Ebrahimi, F. and Salari, E. (2015), "Size-dependent free flexural vibrational behavior of functionally graded nanobeams using semi-analytical differential transform method", *Compos. B*, **79**, 156-169.
Ebrahimi, F. and Salari, E. (2015e), "Thermal buckling and free vibration analysis of size dependent Timoshenko FG nanobeams in thermal environments", *Compos. Struct.*, **128**, 363-380.
Ebrahimi, F. and Salari, E. (2015), "Thermal buckling and free vibration analysis of size dependent Timoshenko FG nanobeams in thermal environments", *Compos. Struct.*, **128**, 363-380.
Ebrahimi, F. and Salari, E. (2015f), "Thermo-mechanical vibration analysis of nonlocal temperature-dependent FG nanobeams with various boundary conditions", *Compos. B*, **78**, 272-290.
Ebrahimi, F. and Salari, E. (2015), "Thermo-mechanical vibration analysis of nonlocal temperature-dependent FG nanobeams with various boundary conditions", *Compos. B*, **78**, 272-290.
Ebrahimi, F. and Barati, M.R. (2016), "An exact solution for buckling analysis of embedded piezoelectro-magnetically actuated nanoscale beams", *Adv. Nano Res.*, **4**(2), 65-84.
Ebrahimi, F. and Barati, M.R. (2016a), "Magneto-electro-elastic buckling analysis of nonlocal curved nanobeams", *Eur. Phys. J. Plus*, **131**(9), 346.
Ebrahimi, F., & Barati, M. R. (2016b). Static stability analysis of smart magneto-electro-elastic heterogeneous nanoplates embedded in an elastic medium based on a four-variable refined plate theory. Smart Materials and Structures, 25(10), 105014.
Ebrahimi, F. and Barati, M.R. (2016c), "Temperature distribution effects on buckling behavior of smart heterogeneous nanosize plates based on nonlocal four-variable refined plate theory", *J. Smart Nano Mater.*, 1-25.
Ebrahimi, F. and Barati, M.R. (2016d), "An exact solution for buckling analysis of embedded piezoelectro-magnetically actuated nanoscale beams", *Adv. Nano Res.*, **4**(2), 65-84.
Ebrahimi, F. and Barati, M.R. (2016e), "Buckling analysis of smart size-dependent higher order magneto-electro-thermo-elastic functionally graded nanosize beams", *J. Mech.*, 1-11.
Ebrahimi, F. and Barati, M.R. (2016f), "A nonlocal higher-order shear deformation beam theory for vibration analysis of size-dependent functionally graded nanobeams", *Arab. J. Sci. Eng.*, **41**(5), 1679-1690.
Ebrahimi, F. and Barati, M.R. (2016g), "Vibration analysis of smart piezoelectrically actuated nanobeams subjected to magneto-electrical field in thermal environment", *J. Vibr. Contr.*, 1077546316646239.
Ebrahimi, F. and Barati, M.R. (2016h), "Buckling analysis of nonlocal third-order shear deformable functionally graded piezoelectric nanobeams embedded in elastic medium", *J. Brazil. Soc. Mech. Sci. Eng.*, 1-16.
Ebrahimi, F. and Barati, M.R. (2016i), "Small scale effects on hygro-thermo-mechanical vibration of temperature dependent nonhomogeneous nanoscale beams", *Mech. Adv. Mater. Struct.*, In press.
Ebrahimi, F. and Barati, M.R. (2016j), "Dynamic modeling of a thermo-piezo-electrically actuated nanosize beam subjected to a magnetic field", *Appl. Phys. A*, **122**(4), 1-18.
Ebrahimi, F. and Barati, M.R. (2016k), "Magnetic field effects on buckling behavior of smart size-dependent graded nanoscale beams", *Eur. Phys. J. Plus*, **131**(7), 1-14.
Ebrahimi, F. and Barati, M.R. (2016l), "Vibration analysis of nonlocal beams made of functionally graded material in thermal environment", *Eur. Phys. J. Plus*, **131**(8), 279.

Ebrahimi, F. and Barati, M.R. (2016m), “A nonlocal higher-order refined magneto-electro-viscoelastic beam model for dynamic analysis of smart nanostructures”, *J. Eng. Sci.*, **107**, 183-196.
Ebrahimi, F. and Barati, M.R. (2016n), “Small-scale effects on hygro-thermo-mechanical vibration of temperature-dependent nonhomogeneous nanoscale beams”, *Mech. Adv. Mater. Struct.*, 1-13.
Ebrahimi, F. and Barati, M.R. (2016o), “A unified formulation for dynamic analysis of nonlocal heterogeneous nanobeams in hygro-thermal environment”, *Appl. Phys. A*, **122**(9), 792.
Ebrahimi, F. and Barati, M.R. (2016p), “Electromechanical buckling behavior of smart piezoelectrically actuated higher-order size-dependent graded nanoscale beams in thermal environment”, *J. Smart Nano Mater.*, **7**(2), 69-90.
Ebrahimi, F. and Barati, M.R. (2016q), “Wave propagation analysis of quasi-3D FG nanobeams in thermal environment based on nonlocal strain gradient theory”, *Appl. Phys. A*, **122**(9), 843.
Ebrahimi, F. and Barati, M.R. (2016r), “Flexural wave propagation analysis of embedded S-FGM nanobeams under longitudinal magnetic field based on nonlocal strain gradient theory”, *Arab. J. Sci. Eng.*, 1-12.
Ebrahimi, F. and Barati, M.R. (2016s), “On nonlocal characteristics of curved inhomogeneous Euler–Bernoulli nanobeams under different temperature distributions”, *Appl. Phys. A*, **122**(10), 880.
Ebrahimi, F. and Barati, M.R. (2016t), “Buckling analysis of piezoelectrically actuated smart nanoscale plates subjected to magnetic field”, *J. Intell. Mater. Syst. Struct.*, 1045389X16672569.
Ebrahimi, F. and Barati, M.R. (2016u), “Size-dependent thermal stability analysis of graded piezomagnetic nanoplates on elastic medium subjected to various thermal environments”, *Appl. Phys. A*, **122**(10), 910.
Ebrahimi, F. and Barati, M.R. (2016v), “Magnetic field effects on dynamic behavior of inhomogeneous thermo-piezo-electrically actuated nanoplates”, *J. Brazil. Soc. Mech. Sci. Eng.*, 1-21.
Ebrahimi, F. and Barati, M.R. (2017a), “Hygrothermal effects on vibration characteristics of viscoelastic FG nanobeams based on nonlocal strain gradient theory”, *Compos. Struct.*, **159**, 433-444.
Ebrahimi, F. and Barati, M.R. (2017b), “A nonlocal strain gradient refined beam model for buckling analysis of size-dependent shear-deformable curved FG nanobeams”, *Compos. Struct.*, **159**, 174-182.
Ebrahimi, F. and Hosseini, S.H.S. (2016a), “Double nanoplate-based NEMS under hydrostatic and electrostatic actuations”, *Euro. Phys. J. Plus*, **131**(5), 1-19.
Ebrahimi, F. and Hosseini, S.H.S. (2016b), “Nonlinear electroelastic vibration analysis of NEMS consisting of double-viscoelastic nanoplates”, *Appl. Phys. A*, **122**(10), 922.
Ebrahimi, F. and Hosseini, S.H.S. (2016c), “Thermal effects on nonlinear vibration behavior of viscoelastic nanosize plates”, *J. Therm. Stress.*, **39**(5), 606-625.
Ebrahimi, F. and Mokhtari, M. (2015), “Transverse vibration analysis of rotating porous beam with functionally graded microstructure using the differential transform method”, *J. Brazil. Soc. Mech. Sci. Eng.*, **37**(4), 1435-1444.
Ebrahimi, F. and Nasirzadeh, P. (2015), “A nonlocal Timoshenko beam theory for vibration analysis of thick nanobeams using differential transform method”, *J. Theoret. Appl. Mech.*, **53**(4), 1041-1052.
Ebrahimi, F. and Salari, E. (2015a), “Size-dependent thermo-electrical buckling analysis of functionally graded piezoelectric nanobeams”, *Smart Mater. Struct.*, **24**(12), 125007.
Ebrahimi, F. and Salari, E. (2015b), “Nonlocal thermo-mechanical vibration analysis of functionally graded nanobeams in thermal environment”, *Acta Astronaut.*, **113**, 29-50.
Ebrahimi, F. and Salari, E. (2016), “Effect of various thermal loadings on buckling and vibrational characteristics of nonlocal temperature-dependent functionally graded nanobeams”, *Mech. Adv. Mater. Struct.*, **23**(12), 1379-1397.
Ebrahimi, F. and Zia, M. (2015), “Large amplitude nonlinear vibration analysis of functionally graded Timoshenko beams with porosities”, *Acta Astronaut.*, **116**, 117-125.
Ebrahimi, F., Barati, M.R. and Haghi, P. (2017), “Thermal effects on wave propagation characteristics of rotating strain gradient temperature-dependent functionally graded nanoscale beams”, *J. Therm. Stress.*, **40**(5), 535-547.
Ebrahimi, F., Ghadiri, M., Salari, E., Hoseini, S.A.H. and Shaghaghi, G.R. (2015b), “Application of the differential transformation method for nonlocal vibration analysis of functionally graded nanobeams”, *J.*

Mech. Sci. Technol., **29**, 1207-1215.
Ebrahimi, F., Ghadiri, M., Salari, E., Hoseini, S.A.H. and Shaghaghi, G.R. (2015)m "Application of the differential transformation method for nonlocal vibration analysis of functionally graded nanobeams", *J. Mech. Sci. Technol.*, **29**, 1207-1215.
Ebrahimi, F., Ghasemi, F. and Salari, E. (2016a), "Investigating thermal effects on vibration behavior of temperature-dependent compositionally graded euler beams with porosities", *Meccan.*, **51**(1), 223-249.
Ebrahimi, F., Naei, M.H. and Rastgoo, A. (2009b), "Geometrically nonlinear vibration analysis of piezoelectrically actuated FGM plate with an initial large deformation", *J. Mech. Sci. Technol.*, **23**(8), 2107-2124.
Ebrahimi, F., Rastgoo, A. and Kargarnovin, M.H. (2008), "Analytical investigation on axisymmetric free vibrations of moderately thick circular functionally graded plate integrated with piezoelectric layers", *J. Mech. Sci. Technol.*, **22**(6), 1058-1072.
Ebrahimi, F., Salari, E. and Hosseini, S.A.H. (2015), "Thermomechanical vibration behavior of FG nanobeams subjected to linear and non-linear temperature distributions", *J. Therm. Stress.*, **38**(12), 1360-1386.
Ebrahimi, F., Salari, E. and Hosseini, S.A.H. (2016c), "In-plane thermal loading effects on vibrational characteristics of functionally graded nanobeams", *Meccan.*, **51**(4), 951-977.
Eltaher, M.A., Emam, S.A. and Mahmoud, F.F. (2012), "Free vibration analysis of functionally graded size-dependent nanobeams", *Appl. Math. Comput.*, **218**, 7406-7420.
Eringen, A.C. (1983), "On differential equations of nonlocal elasticity and solutions of screw dislocation and surface waves", *J. Appl. Phys.*, **54**, 4703-4710.
Fallah, A. and Aghdam, M.M. (2012), "Thermo-mechanical buckling and nonlinear free vibration analysis of functionally graded beams on nonlinear elastic foundation", *Compos. B*, **43**, 1523-1530.
Hosseini-Hashemi, S., Nahas, I., Fakher, M. and Nazemnezhad, R. (2014), "Surface effects on free vibration of piezoelectric functionally graded nanobeams using nonlocal elasticity", *Acta Mech.*, **225**, 1555-1564.
Iijima, S. (1991), "Helical microtubules of graphitic carbon", *Nat.*, **354**(6348), 56-58.
Li, L. and Hu, Y. (2017), "Post-buckling analysis of functionally graded nanobeams incorporating nonlocal stress and microstructure-dependent strain gradient effects", *J. Mech. Sci.*, **120**, 159-170.
Li, L. and Hu, Y. (2017), "Torsional vibration of bi-directional functionally graded nanotubes based on nonlocal elasticity theory", *Compos. Struct.*, **172**, 242-250.
Li, L., Li, X. and Hu, Y. (2016), "Free vibration analysis of nonlocal strain gradient beams made of functionally graded material", *J. Eng. Sci.*, **102**, 77-92.
Nazemnezhad, R. and Hosseini-Hashemi, S. (2014), "Nonlocal nonlinear free vibration of functionally graded nanobeams", *Compos. Struct.*, **110**, 192-199.
Peddieson, J., Buchanan, G.R. and McNitt, R.P. (2003), "Application of nonlocal continuum models to nanotechnology", *J. Eng. Sci.*, **41**(3), 305-312.
Pradhan, S.C. and Murmu, T. (2010), "Application of nonlocal elasticity and DQM in the flapwise bending vibration of a rotating nanocantilever", *Phys. E*, **42**, 1944-1949.
Rahmani, O. and Pedram, O. (2014), "Analysis and modeling the size effect on vibration of functionally graded nanobeams based on nonlocal Timoshenko beam theory", *J. Eng. Sci.*, **77**, 55-70.
Reddy, J.N. (2007), "Nonlocal theories for bending, buckling and vibration of beams", *J. Eng. Sci.*, **45**, 288-307.
Sahmani, S., Aghdam, M.M. and Bahrami, M. (2015), "On the free vibration characteristics of postbuckled third-order shear deformable FGM nanobeams including surface effects", *Compos. Struct.*, **121**, 377-385.
Şimşek, M. (2014), "Large amplitude free vibration of nanobeams with various boundary conditions based on the nonlocal elasticity theory", *Compos. B*, **56**, 621-628.
Thai, H.T. (2012), "A nonlocal beam theory for bending, buckling, and vibration of nanobeams", *J. Eng. Sci.* **52**, 56-64.
Touratier, M. (1991), "An efficient standard plate theory", *J. Eng. Sci.*, **29**, 901-916.
Wang, L. and Hu, H. (2005), "Flexural wave propagation in single-walled carbon nanotubes", *Phys. Rev. B*, **71**, 195412.

Wang, Q. and Liew, K.M. (2007), "Application of nonlocal continuum mechanics to static analysis of micro- and nano-structures", *Phys. Lett. A*, **363**, 236-242.
Wattanasakulpong, N., Gangadhara Prusty, B. and Kelly, D.W. (2011), "Thermal buckling and elastic vibration of third-order shear deformable functionally graded beams", *J. Mech. Sci.*, **53**, 734-743.
Zenkour, A.M., Abouelregal, A.E., Alnefaie, K.A., Abu-Hamdeh, N.H. and Aifantis, E.C. (2014), "A refined nonlocal thermoelasticity theory for the vibration of nanobeams induced by ramp-type heating", *Appl. Math. Comput.*, **248**, 169-183.
Zhang, Y.Q., Liu, G.R. and Xie, X.Y. (2005), "Free transverse vibrations of double-walled carbon nanotubes using a theory of nonlocal elasticity", *Phys. Rev. B*, **71**, 195404.

OP